crystals

MDPI

*Review*

# Metal–Organic Framework for Plastic Depolymerization and Upcycling

**Kisung Lee [1,†], Sumin Han [1,†], Minse Kim [1,2], Byoung-su Kim [1,2], Jeong-Ann Park [3], Kwang Suk Lim [1,2,4], Suk-Jin Ha [1,2,4] and Hyun-Ouk Kim [1,2,4,*]**

1 Division of Chemical Engineering and Bioengineering, College of Art, Culture and Engineering, Kangwon National University, Chuncheon 24341, Gangwon-do, Republic of Korea; dlrltjd0623@kangwon.ac.kr (K.L.); sumin1646@kangwon.ac.kr (S.H.); minse0415@kangwon.ac.kr (M.K.); dhenrl99@kangwon.ac.kr (B.-s.K.); kslim@kangwon.ac.kr (K.S.L.); sjha@kangwon.ac.kr (S.-J.H.)
2 Department of Smart Health Science and Technology, Kangwon National University, Chuncheon 24341, Gangwon-do, Republic of Korea
3 Department of Environmental Engineering, College of ACE, Kangwon National University, Chuncheon 24341, Gangwon-do, Republic of Korea; pjaan@kangwon.ac.kr
4 Institute of Fermentation of Brewing, Kangwon National University, Chuncheon 24341, Gangwon-do, Republic of Korea
* Correspondence: kimhoman@kangwon.ac.kr; Tel.: +82-33-250-6272
† These authors contributed equally to this work.

**Abstract**

Plastics are essential in modern life but accumulate as waste. Mechanical reprocessing reduces material quality, whereas thermochemical routes require harsh conditions and are costly to upgrade. Together, these factors hinder the large-scale recovery of plastics into equivalent materials. Metal–organic frameworks provide a programmable platform where reticular design fixes porosity and positions well-defined Lewis, Brønsted, redox, and photoredox sites that can preconcentrate oligomers and align scissile bonds for activation. These attributes enable complementary pathways spanning hydrolysis, alcoholysis, aminolysis, photo-oxidation, electrocatalysis, and MOF-derived transformations, with adsorption-guided capture-to-catalysis workflows emerging as integrative schemes. In this review, we establish common figures of merit such as space–time yield, monomer selectivity and purity, energy intensity, site-normalized turnover, and solvent or corrosion footprints. These metrics are connected to design rules that involve active-site chemistry and transport through semi-crystalline substrates. We also emphasize durability under hot aqueous, alcoholic, or oxidative conditions as essential for producing polymer-grade products.

**Keywords:** metal–organic frameworks (MOFs); plastic depolymerization; upcycling; environment pollution; circular economy

check for updates

Academic Editor: Yusuf Valentino Kaneti

Received: 19 August 2025
Revised: 7 October 2025
Accepted: 13 October 2025
Published: 16 October 2025

**Citation:** Lee, K.; Han, S.; Kim, M.; Kim, B.-s.; Park, J.-A.; Lim, K.S.; Ha, S.-J.; Kim, H.-O. Metal–Organic Framework for Plastic Depolymerization and Upcycling. *Crystals* **2025**, *15*, 897. https://doi.org/10.3390/cryst15100897

**Copyright:** © 2025 by the authors. Licensee MDPI, Basel, Switzerland. This article is an open access article distributed under the terms and conditions of the Creative Commons Attribution (CC BY) license (https://creativecommons.org/licenses/by/4.0/).

## 1. Introduction

Many reviews on plastic recycling have appeared in recent years, but most focus only on conventional thermochemical or catalytic routes. They rarely integrate performance benchmarks, engineering considerations, or environmental and techno-economic analyses. This review emphasizes these aspects as central to the discussion.

Mechanical reprocessing can compromise plastic quality and is sensitive to contamination, as well as multilayer packaging. Thermochemical routes, such as pyrolysis or gasification, require high temperatures and produce complex mixtures that need costly

upgrading [1,2]. We use this thermochemical landscape as the baseline for benchmarking MOF strategies (Figure 1). Consequently, only a small fraction of plastics is reclaimed as like-for-like feedstock; the rest is landfilled, incinerated, or leaked as macro- and microplastics [3,4]. To overcome this imbalance, catalysts are needed that can break down polymers with molecular precision under mild conditions. They should also provide monomers or higher-value products on demand and function with mixed waste streams without costly separation steps [5].

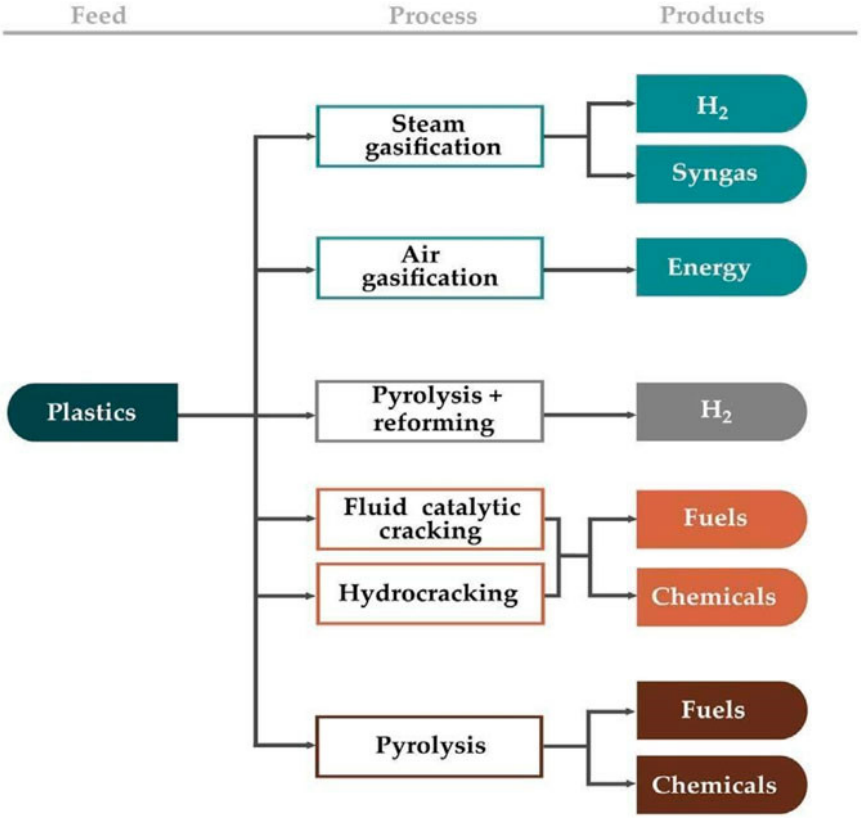



**Figure 1.** Conventional thermochemical pathways for plastic valorization. Process map summarizing gasification (steam/air), pyrolysis ± reforming, and refinery routes (fluid catalytic cracking and hydrocracking) and their dominant product classes. This baseline is used to benchmark MOF-enabled depolymerization in terms of severity and selectivity. Reproduced from [1], licensed under CC BY 4.0, © 2022 H.H. Shah, M. Amin, A. Iqbal, I. Nadeem, M. Kalin, A.M. Soomar, and A.M. Galal.

Metal–organic frameworks (MOFs) are crystalline, porous materials constructed from metal nodes and organic linkers through reticular chemistry. This design enables precise control of topology and functionality [6,7]. MOFs offer very high surface areas, tunable pore sizes, and diverse active sites, making them distinct from conventional porous solids. Over the past two decades, they have been studied for gas storage, separation, sensing, drug delivery, and energy storage, with catalysis emerging as one of their most versatile applications [6,7]. In the context of plastics, these attributes are particularly relevant because MOF pores can pre-concentrate oligomers, organize polymer segments through π–π, electrostatic, or hydrophobic interactions, and position scissile bonds near catalytically active centers [8,9]. Recent discussions have highlighted the potential of MOFs not only to address environmental threats from plastics but also to turn them into opportunities for upcycling into higher-value products [8].

Metal–organic frameworks (MOFs) offer a distinctive platform for such transformations [10]. Reticular chemistry allows the modular assembly of metal nodes and organic linkers into crystalline lattices with programmable porosity, a high internal surface area, and

well-defined, accessible active sites [11]. Lewis/Brønsted acidity, redox, and photoredox functionality can be tuned via node selection, linker electronics, defect engineering, heterometallic nodes, and composites [8]. The same pores that pre-concentrate small molecules can adsorb and organize polymer segments through π–π, electrostatic, and hydrophobic interactions, positioning scissile bonds near catalytic sites; a representative hydrolytic mechanism is illustrated [12] in Figure 2. These attributes have enabled complementary depolymerization modalities—hydrolysis, alcoholysis and aminolysis of polyesters and polyamides under neutral to mildly acidic conditions [13]; photocatalytic pathways (often in MOF–semiconductor hybrids) that generate reactive oxygen species for C–O and C–C scission [14–16]; electro-/photoelectrocatalytic variants that lower thermal budgets [17]; and MOF-derived catalysts that activate otherwise inert backbones [8]. Adsorption-guided "adsorb-to-deconstruct-to-upcycle" workflows, including pre-concentration with MOF membranes, are emerging to couple capture with catalysis [18].

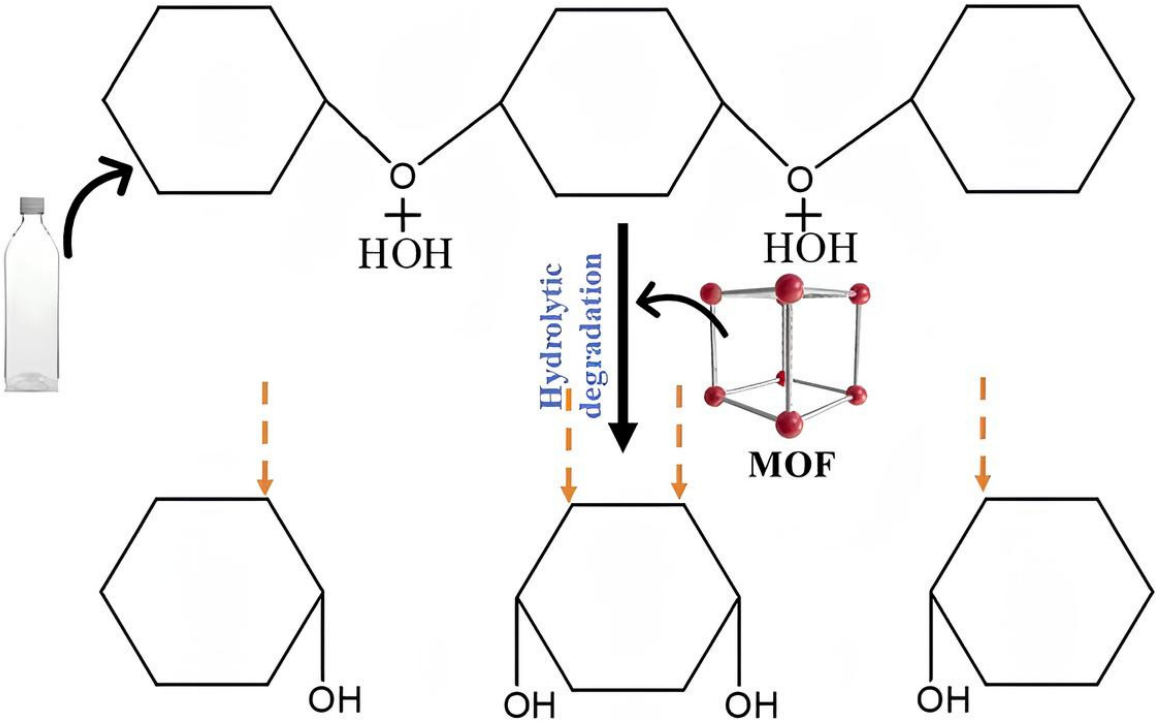



**Figure 2.** MOF-mediated hydrolytic depolymerization of polyester linkages. Schematic depiction of Lewis-acidic nodes (for example, $Zr_6$-oxo clusters) coordinating and activating ester bonds, enabling C–O scission to yield diacids and diols (for PET, terephthalic acid and ethylene glycol) under comparatively mild conditions. Reproduced from [12], licensed under CC BY 4.0, © 2024, with permission from Elsevier.

For practical use, it is essential to control mass transport and interfacial contact between solid catalysts and semi-crystalline polymers. Catalysts should remain stable and recyclable in aqueous, alcoholic, or oxidative environments. They must also resist additives and fillers commonly present in post-consumer plastics [19]. Product streams must meet polymer-grade specifications for true circularity, motivating inline separations and tandem catalysis that directly refine depolymerization outputs [13]. Techno-economic analysis and life-cycle assessment should be integrated at an early stage of the project. Standardized figures of merit—such as space–time yield, monomer selectivity and purity, energy intensity, site-normalized turnover, and solvent or corrosion footprints—are needed to enable fair comparisons [20]. The scope and roadmap of this Review are summarized in Figure 3,

which frames how MOF design principles and mechanisms can uniquely enable circular plastics at relevant scales [18].

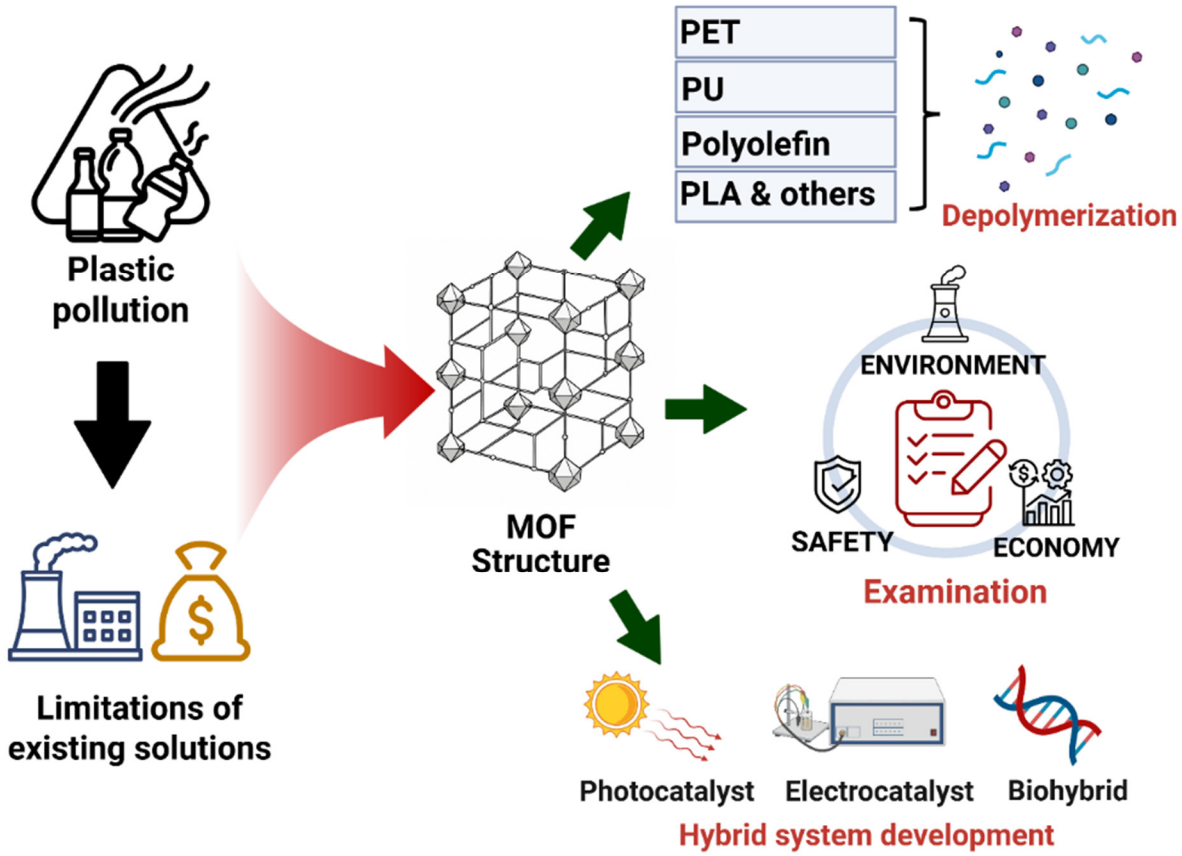



**Figure 3.** Scope and roadmap of MOF-enabled plastic upcycling. Plastic pollution and limitations of incumbent solutions motivate MOF-based strategies. The MOF platform targets diverse polymers (for example, PET, PU, polyolefins, and PLA), while cross-cutting assessment considers environmental footprint, safety, and techno-economics. Hybrid modalities highlighted in this Review include photo-, electro-, and bio-hybrid catalysis.

Previous reviews on plastic recycling have mainly examined the initial steps of conventional thermochemical pathways or catalytic depolymerization. However, they often fail to incorporate performance benchmarks, life-cycle assessments, and techno-economic considerations. This review distinguishes itself by explicitly benchmarking MOF-based depolymerization against conventional thermochemical methods and establishing standardized metrics that link active site chemistry, transport, and durability to the recovery of polymer-grade products. By situating MOFs within the broader recycling landscape, this review provides a comparative and application-oriented framework for achieving true circularity beyond proof-of-concept reports.

## 2. Design Principles of MOF Catalysts for Polymer Depolymerization and Upcycling

### *2.1. Framework Crystallinity, Porosity, and Accessible Surface*

Metal–organic frameworks are crystalline lattices formed by metal nodes and multitopic linkers. They can generate one-dimensional channels, two-dimensional layers, or three-dimensional networks with periodic active sites. In plastic depolymerization and upcycling, the key metrics are surface accessibility under reaction conditions, pore connectivity across different length scales, and structural stability over repeated cycles, rather than headline BET values [8]. Microporous lattices efficiently pre-concentrate small

molecules and water around Lewis-acidic clusters, which promote ester activation. In contrast, semi-crystalline polyolefins require meso- or microporosity, as well as careful control of wettability, to achieve effective interfacial contact [8]. Strategies that increase surface area by creating defects or using templated growth can reduce mechanical strength and hydrolytic stability. Moreover, gravimetric surface area often correlates poorly with volumetric productivity once the materials are formed into pellets or monoliths [21].

Covalent organic frameworks (COFs) provide a useful reticular comparator and can also function as adsorption scaffolds in MOF–COF hybrids. While early imine-linked COFs face hydrolytic stress in depolymerization media, recent advances in frameworks with more robust linkages such as olefin and thiazole demonstrate significantly higher chemical stability. This contrast highlights how lattice connectivity influences durability, with Zr- or Hf-carboxylate MOFs continuing to serve as benchmarks for aqueous stability [13]. Figure 4 shows an imine-linked three-dimensional COF assembly to illustrate connectivity principles. It also highlights that accessibility, transport, and durability ultimately determine the performance limits for catalytic deconstruction at scale [18].

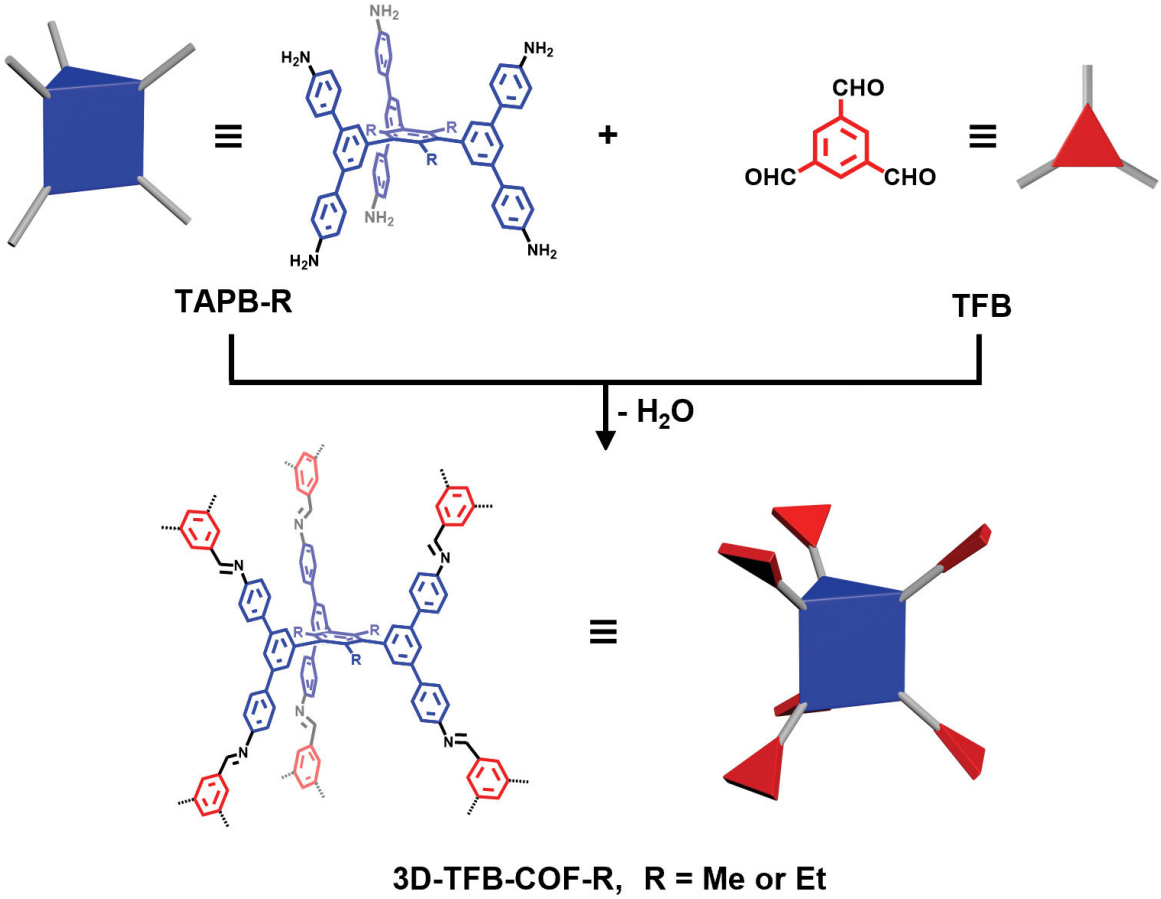



**Figure 4.** Reticular comparator based on animine-linked three-dimensional covalent organic framework. Condensation of an eight-connected triamine node TAPB R with the three-connected aldehyde 1,3,5 triformylbenzene TFB eliminates water to give an extended 3D TFB COF R. The cartoons highlight node–linker connectivity relevant to the design of MOF or MOF COF hybrid architectures for polymer capture and deconstruction. Reproduced from [22], © 2024 American Association for the Advancement of Science. Reproduced with permission.

### *2.2. Coordination Environments and Active-Site Engineering*

In metal–organic frameworks, the metal nodes act as Lewis-acidic centers. They become coordinatively unsaturated when terminal ligands are removed or exchanged. Linker functionalization further adjusts polarity, hydrophobicity, and electron density at

the interface, influencing polymer pre-adsorption and transition-state stabilization [23]. The NU-912 and NU-912(Hf) families illustrate this approach with amine, halogen, and nitrile substituents on the linker. Figure 5 shows that all derivatives, including the bromide form, retain faceted rod-like crystallites rather than assembling into aggregates, consistent with the captional description of NU-912(Hf)-Br. Therefore, activity trends cannot be assigned to electronic effects alone unless comparisons are normalized for surface area, external surface exposure, and diffusion path length [24].

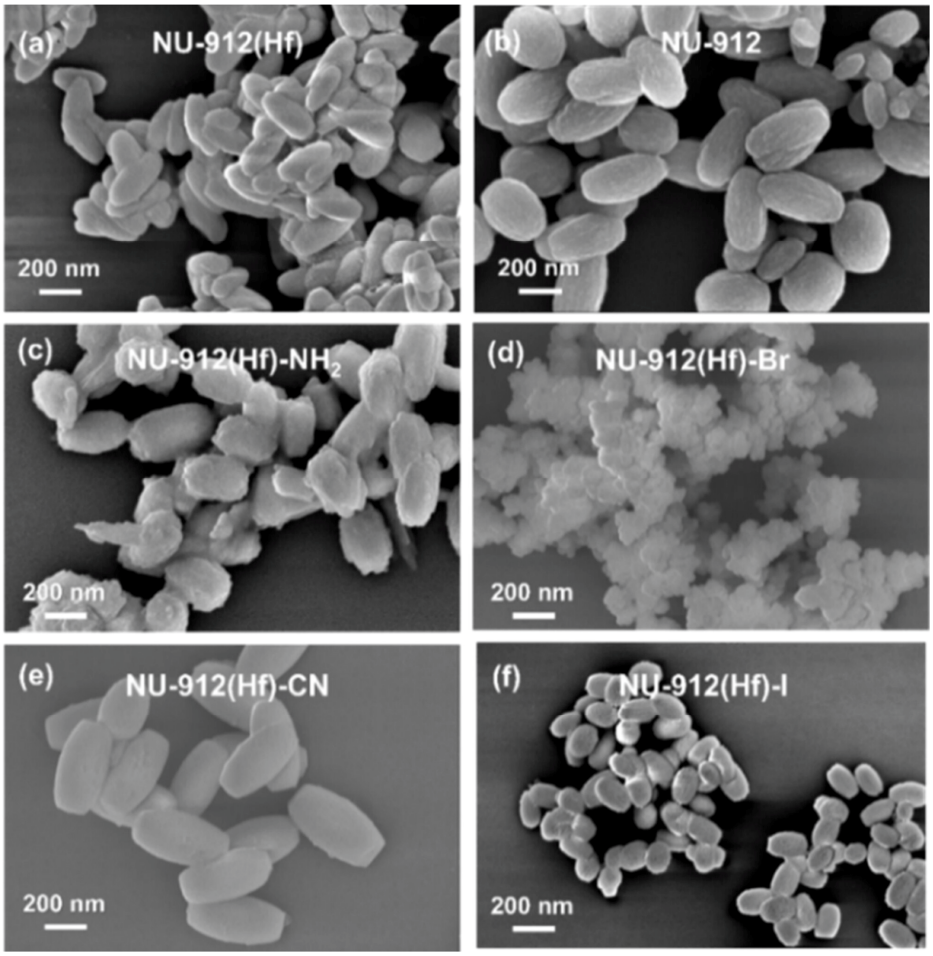



**Figure 5.** Morphology of linker-functionalized NU-912 series. SEM images of NU-912 Hf, NU-912, NU-912 Hf-NH2, NU-912 Hf-Br, NU-912 Hf-CN, and NU-912 Hf-I show similar faceted crystallites. The preserved morphology across substitutions supports comparisons that isolate electronic and interfacial effects on adsorption and catalytic depolymerization performance. (**a**) NU-912(Hf), (**b**) NU-912, (**c**) NU-912(Hf)-$NH_2$, (**d**) NU-912(Hf)-Br, (**e**) NU-912(Hf)-CN, (**f**) NU-912(Hf)-I. Reproduced with permission from [24]. Copyright 2023 American Chemical Society.

Stronger nominal acidity or higher defect density does not necessarily ensure higher turnover when hot water or alcohols compromise hydrolytic robustness, pore connectivity, and mechanical integrity; therefore, prior studies should include site-normalized rates per accessible node, adsorption coefficients for relevant oligomers, and post-reaction retention of porosity and particle morphology [25]. Frustrated Lewis pairs in MOFs are promising for small-molecule activation. However, clear links to polymer bond scission are still scarce. Progress will depend on operando spectroscopy and probe reactions that map node–linker ensembles to scission selectivity, so that material choices are guided by validated mechanisms rather than inference [26].

### *2.3. Stability Under Depolymerization Conditions*

For plastic degradation, the relevant measure of stability is thr retention of active sites and pore connectivity in hot water or alcohols and under oxidants rather than decomposition temperature in inert gas [27]. Zr- and Hf-carboxylate frameworks, including UiO-66 and MOF-808, are benchmarks for hydrolytic stability. Yet, creating too many defects or allowing linker hydrolysis can reduce mechanical strength and even collapse pores. Therefore, strategies to increase nominal acidity must also preserve the durability and recyclability of shaped bodies [28]. Mechanical integrity governs space–time yield once pellets or monoliths undergo swelling, solvent exchange, and shear, and flexible lattices may either dissipate stress or drift into less active configurations. CALF-20 highlights this interplay. It exhibits negative thermal expansion, large elastic strain, and a strain-softening transition that modifies coordination geometry and unit-cell angles. These changes, along with bond strengths and the energy–volume landscape, are summarized in Figure 6 [29].

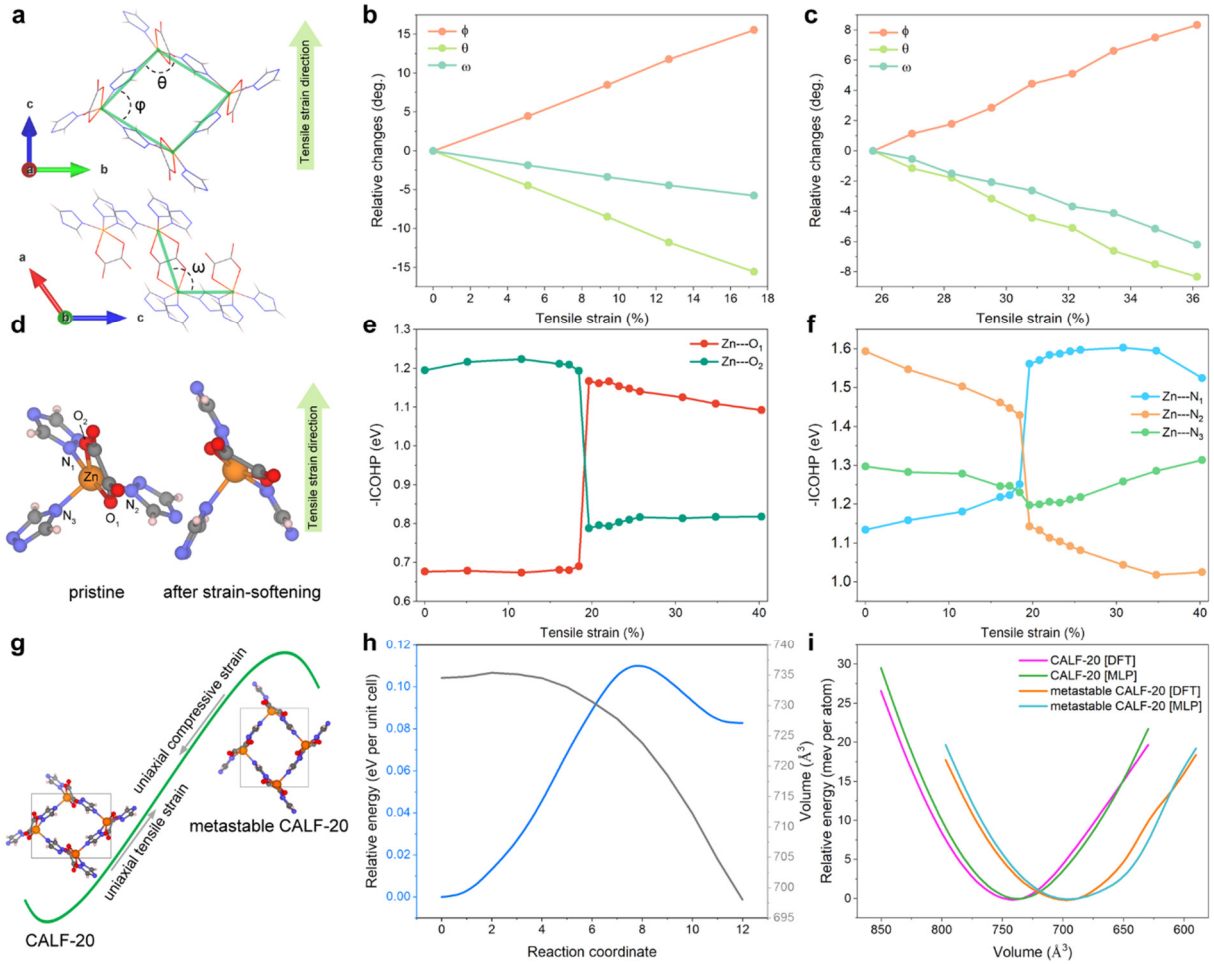



**Figure 6.** Strain-induced phase transition of CALF-20. (**a**) Unit-cell views showing ligand angles phi, theta, and omega along the tensile-strain direction. (**b**,**c**) Relative changes in these angles before and after strain softening under tension along the [001] direction. (**d**) Representative Zn coordination in pristine and strain-softened structures. (**e**,**f**) Evolution of bond-strength indicators for Zn–O and Zn–N with increasing strain. (**g**) Schematic of the transition pathway under uniaxial tension leading to a metastable phase. (**h**) Relative energy (blue line) and volume (gray line) along the transition coordinate. (**i**) Energy–volume curves for pristine and metastable phases from density functional theory and machine-learning potentials. Reproduced with permission from Nature Communications [30], © Springer Nature.

Machine learning potentials are valuable for mapping such transitions. However, they require calibration with operando diffraction and spectroscopy under realistic conditions. Robustness can only be claimed when site-normalized activity retention, post-reaction porosity, and crush strength are demonstrated over many cycles [26]. Frameworks that maintain high accessibility and recoverable mechanics in working media, rather than those that deliver record values measured ex situ, are the most likely to translate to scalable depolymerization and upcycling [24].

### *2.4. Functional Classification of MOF Catalysts for Polymer Deconstruction*

A useful taxonomy groups MOF platforms by bond-breaking modality and reactor reality rather than by metal identity alone. Lewis-acidic Zr or Hf carboxylate nodes promote hydrolysis, alcoholysis, and aminolysis of polyesters and polyamides by coordinating and activating ester or amide linkages. However, near-quantitative yields in prior studies often depend on concentrated nucleophiles, excess solvent, or fine powders; therefore, fair comparisons should use site-normalized rates, product purity, and space–time yield under identical mass-transfer limits [13]. Redox-active and photosensitizing frameworks—such as Fe- or Ti-based systems, linker chromophores, and MOF–semiconductor hybrids—enable oxidative C–O and C–C bond scission. However, their advantages disappear if light penetration, oxygen delivery, and catalyst durability are not properly engineered [25]. Mixed-metal or polyoxometalate composites often claim catalytic synergy. Yet, the observed activity may simply reflect external surface exposure or porosity, rather than real bimetal cooperation. To confirm true effects, rigorous control samples and operando probes are required [31].

Polyolefin conversion rarely occurs within purely hydrolytic windows. In practice, it relies on supported or MOF-derived metal species such as Ru or Ni hydride ensembles or M–N–C motifs. These are coupled with acidity to promote tandem cracking and isomerization while preserving the integrity of the framework [32]. Adsorptive preconcentration using MOF or COF membranes can increase effective rates but should be accompanied by metrics such as flux, fouling resistance, and recyclability [10]. In this functional map, the strongest candidates for scalable depolymerization and upcycling are those platforms that combine hydrolytic or oxidative endurance with retained accessibility. These properties are essential for shaped bodies to perform reliably at scale [19].

As summarized in Table 1, MOF-based catalysts can be functionally categorized into hydrolytic, photocatalytic, adsorptive, and MOF-derived classes. Figure 7 provides a schematic overview of these strategies, highlighting the role of adsorptive preconcentration in coupling capture with catalytic deconstruction and upcycling.

**Table 1.** Functional classification of MOF catalysts for polymer deconstruction.

| Classification (Bond-Breaking Modality) | Representative MOF Types/Metals | Key Function | Target Polymers | Distinctive Features | References |
|---|---|---|---|---|---|
| Hydrolytic/ Alcoholytic/ Aminolytic | Zr- or Hf-carboxylates (e.g., UiO-66 series) | Coordinate and activate ester/ amide linkages | Polyesters (PET), Polyamides (Nylon) | Mild conditions; enables recov ery of pure monomers | [7,13,25] |
| Redox/ Photocatalytic | Fe, Ti frameworks, linker-based chromophores, MOF–semiconductor hybrids | Generate ROS for C–O and C–C bond scission | PET, PLA | Light-driven, tunable selectivity; requires engineered stability and oxygen/light delivery | [14–16] |

**Table 1.** *Cont.*

| Classification (Bond-Breaking Modality) | Representative MOF Types/Metals | Key Function | Target Polymers | Distinctive Features | References |
|---|---|---|---|---|---|
| MOF-derived catalysts | Pyrolyzed M–N–C motifs, Ru/Ni hydride ensembles | Tandem cracking, hydrogenolysis, isomerization | Polyolefins (PE, PP) | Effective for otherwise inert backbones; integrates metal nanoparticle activity | [33] |
| Adsorptive preconcentration | MOF/COF membranes, defect-rich frameworks | Capture and concentrate oligomers prior to catalytic cleavage | Mixed waste streams | "Adsorb-to-deconstruct-to-upcycle" workflow; enhances mass transport efficiency | [10,18,19] |

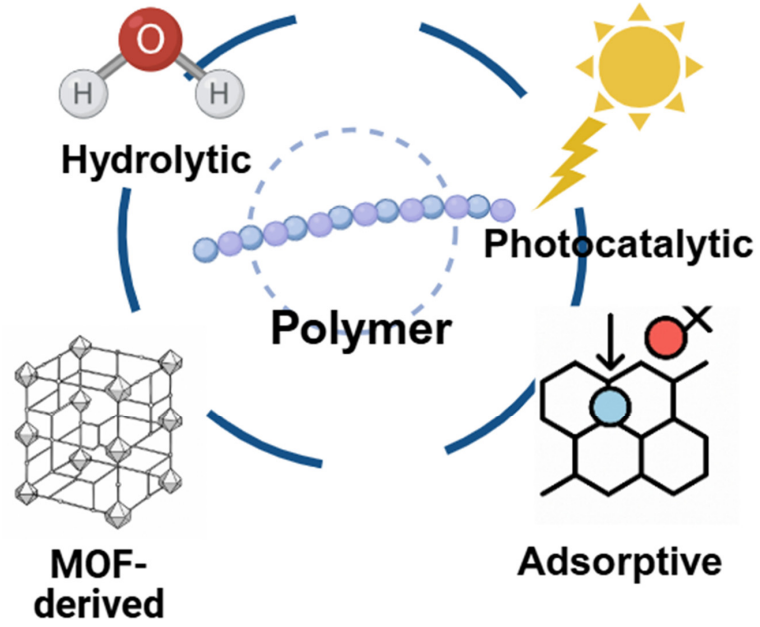



**Figure 7.** Schematic representation of MOF-based strategies for plastic depolymerization and upcycling. This schematic illustrates four major MOF-related pathways for polymer degradation and upcycling. Hydrolytic MOFs promote ester or amide bond cleavage in the presence of water. Photocatalytic MOFs harvest light to generate reactive oxygen species that can break C–O or C–C bonds. Adsorptive MOFs selectively capture and preconcentrate polymer fragments or additives within porous frameworks to facilitate bond activation. MOF-derived materials utilize metal or carbonaceous species obtained from pyrolyzed MOFs to catalyze polymer breakdown. Together, these approaches highlight the versatility of MOFs and their derivatives in addressing plastic waste valorization.

Compared to existing catalysts already utilized on an industrial scale, such as zeolites, activated carbon, and metal oxides, MOFs remain in the early stages of commercialization. MOFs are widely studied for polymer degradation and upcycling. Their reticular structures, modular pores, and combined adsorption–catalysis functions make them highly versatile. In contrast to zeolites and oxides, which excel under harsh pyrolysis or oxidation conditions, MOFs allow selective bond cleavage under mild conditions and can couple capture with conversion. These distinctive properties are increasingly positioning MOFs as a promising alternative for future scalable plastic upcycling [8,11,25].

The catalytic performance of MOFs in plastic depolymerization is governed by several interrelated structural and mechanistic factors. Pore topology and aperture size determine whether polymer chains can diffuse into the framework and approach the active centers, while surface area and hierarchical porosity control mass-transfer limitations. The coor-

dination environment and oxidation state of metal nodes, together with the electronic properties of organic linkers, dictate the type and strength of bond activation—such as hydrolytic, oxidative, or photocatalytic cleavage. Defect density and the presence of open metal sites often enhance nucleophilic attack or radical formation, but may also reduce structural stability under humid or oxidative conditions. Furthermore, adsorption interactions, including π–π stacking, hydrogen bonding, and electrostatic attraction between polymer fragments and pore walls, can pre-concentrate substrates and facilitate coupled adsorption–reaction pathways. Collectively, these factors define the efficiency, selectivity, and recyclability of MOF-based catalysts in polymer deconstruction and upcycling under mild conditions. [7,8,11,34–37].

## 3. Scalable Manufacturing and Functionalization of MOF Catalysts

### *3.1. Synthesis Routes and Scale-Up Considerations*

Solvothermal synthesis is still the standard method for producing highly crystalline MOFs, but it is solvent-intensive and slow [8]. Microwave heating offers faster nucleation and shorter reaction times. However, it often produces smaller crystallites with more defects, which can exaggerate apparent activity while lowering hydrolytic stability and mechanical strength [38]. Mechanochemical routes minimize solvent use and can lower the E-factor, although milling can introduce microstrain and broaden pore distributions that complicate transport during depolymerization [39]. Continuous-flow reactors improve reproducibility and throughput but should include space–time yield alongside particle size, defect density, and post-reaction robustness so that cross-route comparisons are meaningful [38]. Figure 8 presents the 13C solid-state NMR of CALF-20 prepared by both solvothermal and microwave routes. Conserved chemical shifts show that the framework connectivity is retained, while line-shape changes reveal variations in defect populations or residual species. When combined with site-normalized rates and activity retention after cycling, these diagnostics help identify synthesis routes that genuinely improve plastic degradation and upcycling instead of merely maximizing surface area or yield [40].

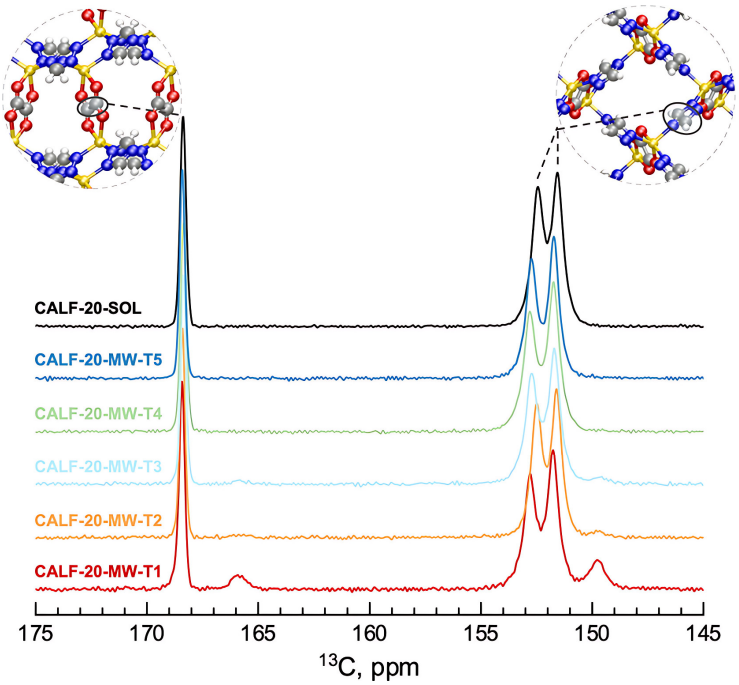



**Figure 8.** 13C solid-state NMR spectra of CALF-20 prepared by solvothermal and microwave routes. Spectra for CALF-20-SOL and CALF-20-MW series display comparable carbon environments that

indicate preserved framework connectivity, with subtle line-shape differences consistent with variations in defect population or residual species. Insets depict representative local coordination environments used to guide interpretation. Reproduced from [41], licensed under CC BY-NC-ND 4.0, © 2025 Daniel Pereira, Mariana Sardo, Ricardo Vieira, Ildefonso Marín-Montesinos, and Luís Mafra.

### *3.2. Sustainable and Scalable Manufacturing*

Water-based routes, continuous-flow reactors, and solvent-free or solvent-minimal methods promise lower hazards and higher throughput for MOF production. However, claims of greenness or scalability are valid only when productivity and material quality are reported together with full process footprints [42]. Aqueous syntheses that replace DMF can provide high isolated yields with space–time yields of several hundred kilograms per cubic meter per day. Under favorable dual-ligand conditions with mild acetate modulators, reported values increase to tens of tons per cubic meter per day [43]. For the CPO-27 series, room-temperature preparations have achieved space–time yields in the tens of thousands of kilograms per cubic meter per day [34]. These figures are meaningful only if parameters such as crystallite size distribution, defect density, residual salts, filterability, drying energy, and waste neutralization are properly quantified. Rapid nucleation can otherwise inflate defect populations, which may increase apparent activity but reduce hydrolytic stability and hinder the shaping of materials into pellets or monoliths [35].

Mechanochemical and microwave-assisted routes reduce solvent or time but can introduce microstrain and broadened pore distributions that complicate mass transport during depolymerization [44]. Flow chemistry can enhance reproducibility and allow solvent recycling. However, it requires careful control of mixing, heat removal, and corrosion caused by halides or acids. To assess performance fairly, metrics should also include solvent and water consumption per kilogram of product, total energy intensity, reuse of mother liquor, and site-normalized activity retention after repeated catalytic cycles [45]. Manufacturing strategies that pair high space–time yield with durable porosity and mechanical integrity in shaped bodies are the ones most likely to translate MOF catalysts to practical plastic degradation and upcycling [42,46].

### *3.3. Post-Synthetic Functionalization and Active-Site Modulation*

Post-synthetic routes expand MOF reactivity through strategies such as ligand exchange, defect installation, grafting donor or acceptor groups, linker metalation, and redox tuning. These modifications create cooperative acid–base and adsorptive microenvironments that pre-organize polymer segments for bond activation [47]. These treatments can sharpen selectivity and enable tandem functions that are difficult to achieve during synthesis. However, their benefits often involve trade-offs that ultimately determine their practical value in depolymerization and upcycling [48]. Pore blocking by bulky grafts, loss of hydrolytic stability after defect creation, and microstrain from ligand exchange can reduce accessibility and weaken shaped bodies. These effects occur even when apparent activity increases in small-scale tests [36]. Pore blocking by bulky grafts, loss of hydrolytic stability after defect creation, and microstrain from ligand exchange can reduce accessibility and weaken shaped bodies. These effects appear even when small-scale tests suggest higher apparent activity [37].

Comparisons across modifications are valid only when normalized to the number of accessible active sites. To be reliable, they should also report adsorption coefficients for relevant oligomers and product purity. In addition, the retention of porosity and crystallinity after cycling, as well as the crush strength of pellets or monoliths, must be documented [46,49,50]. The most effective strategies are those that combine durable microenvironments, preserved transport across hierarchical pores, and reproducible per-

formance on mixed post-consumer feeds. Progress depends on these factors rather than simply maximizing graft density or gravimetric surface area [51].

### 3.4. Recent Trends in the Utilization of MOF-Based Materials for Plastic Depolymerization and Upcycling

Over the past decade, MOF-based systems have witnessed a rapid expansion of applications in plastic depolymerization and upcycling. Early work primarily focused on the hydrolytic depolymerization of polyesters such as PET and PU, using Zr- and Hf-based frameworks (e.g., UiO-type MOFs), demonstrating remarkable activity under mild conditions compared to conventional metal oxides or zeolites [25]. In parallel, photocatalytic and oxidative strategies using Fe-, Ti-, and Ce-containing MOFs have been developed for polyolefins and polyethylene-like substrates. These approaches address challenges that were once limited to high-temperature pyrolysis [9,25]. More recent studies highlight two emerging directions. First, hybrid MOF composites (MOFs combined with enzymes, nanoparticles, or polymers) have been engineered to enhance stability and broaden the scope to mixed or contaminated waste streams [52,53]. Second, MOF-derived catalysts, obtained via controlled pyrolysis of MOFs to produce porous metal oxides or carbons, have shown promise for upcycling polyolefins into liquid fuels and valuable chemicals under scalable conditions [8,9]. Despite these advances, most studies remain at the proof-of-concept stage, often relying on model plastics or highly controlled laboratory conditions. Standardized activity metrics, long-term durability assessments, and validation under realistic post-consumer plastic streams are still urgently required. Collectively, these trends indicate that MOFs are moving beyond niche laboratory demonstrations to broader consideration as versatile platforms for future scalable plastic upcycling.

## 4. Mechanistic Basis of MOF-Mediated Plastic Degradation

### 4.1. Polymer Adsorption and Diffusion in MOF Pores

Polymer uptake in MOFs is controlled by pore-size distribution, connectivity, and interfacial chemistry. These factors determine the balance between enthalpic binding and entropic penalties for chain confinement. Strong adsorption can help preconcentrate oligomers near Lewis-acidic nodes, but overbinding and narrow pores restrict transport and slow down product release [6]. Molecular-dynamics isotherms for acidic gases in MIL-100(Fe) (Figure 9) reveal that strong adsorption does not always lead to fast mobility. $H_2S$ is unusual in that it shows both strong interactions and high calculated diffusivity. This suggests that adsorption design should focus on intermediate binding energies and hierarchical transport pathways rather than maximizing heats of adsorption [6,25].

Earlier studies showed that MOF stationary phases can recognize polymers and capture microplastics with high capacity. Yet, in complex media, their performance often drops because of ionic strength, natural organic matter, and competitive adsorption. To evaluate reliability, metrics should also report rate constants for relevant oligomers, partition coefficients in water or alcohols, breakthrough capacities under flow, and retention of porosity and particle integrity after cycling [6,7]. For catalytic depolymerization, the most effective materials combine moderate binding with fast diffusion, wettable meso- or macropore access, and resilience to fouling. Comparisons should be normalized to accessible surface area and external surface exposure so that observed trends reflect microenvironment and topology rather than particle size alone [33].

Although adsorption and diffusion studies demonstrate promising preconcentration effects, most experiments use model oligomers or single-component systems. These do not capture the complexity of real plastic waste streams containing additives, dyes, and

heterogeneous crystallinity. Future studies should benchmark adsorption and diffusion under realistic polymer feeds and flow conditions [8].

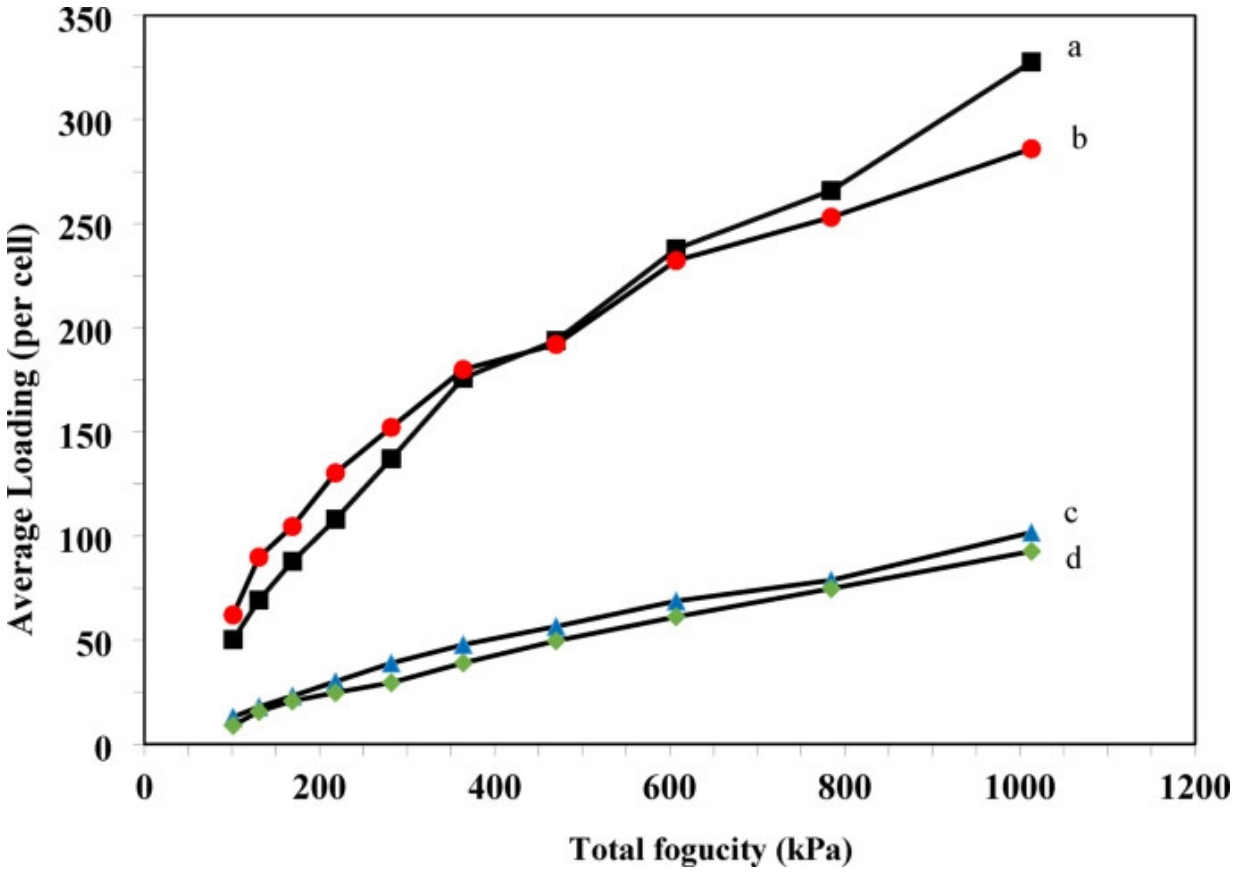



**Figure 9.** Adsorption isotherms for MIL-100(Fe) from molecular dynamics. (**a**) $H_2S$ (**b**) $SO_2$ (**c**) $NO_2$ (**d**) $CO_2$. Distinct uptake profiles reflect differing framework affinities and transport characteristics relevant to preconcentration and mass transfer. Simulations employed the COMPASS force field with Ewald electrostatics and atom-based van der Waals interactions at 298.15 K, 101.3–1013 kPa (9 fugacity steps), using NVT (100 ns, 1 fs) followed by NVE (100 ns, 1 fs) ensembles. Adapted from [54], licensed under CC BY 4.0, © 2025 by the authors.

### *4.2. Nucleophilic Scission Pathways*

Hydrolysis, alcoholysis, and aminolysis in MOFs proceed by nucleophilic attack on ester or amide groups activated at $Zr_6$ or $Hf_6$ nodes. Pore polarity and solvent activity influence the transition state and product release. Yet, many prior studies that claim near-quantitative PET conversion rely on harsh conditions such as high temperature, excess nucleophiles, fine powders, and short diffusion paths. Meaningful comparisons must therefore normalize rates to accessible sites, specify polymer-to-reagent ratios, and provide data on monomer purity and space–time yield under identical mass-transfer limits [25,33,55]. Alcoholysis is attractive because volatile pairs, such as dimethyl terephthalate with methanol or bis-hydroxyethyl terephthalate with ethylene glycol, simplify product separation. However, claims of exceptional activity on vacancy-rich oxides or MOF composites require hot-filtration and leaching controls to rule out contributions from dissolved species [55]. Aminolysis enables upcycling to terephthalamides, but strongly coordinating products and salts can poison the catalytic nodes. Therefore, catalyst reuse, pore accessibility, and adsorption coefficients for relevant oligomers should be monitored alongside conversion [56,57].

The best-performing frameworks strike a balance between adsorption and mobility. They do this by combining Lewis acidity with wettable meso- or macropore pathways,

instead of only maximizing gravimetric surface area. In addition, their durability must be proven in hot aqueous or alcoholic media, with porosity, particle integrity, and crush strength maintained in shaped bodies [7,33]. Enzyme–MOF ensembles can provide lower-severity routes when enzymes are immobilized within protective microenvironments. However, the benefits are meaningful only if activity retention, partitioning in complex feeds, and compatibility with downstream upgrading are demonstrated [33]. Overall, platforms that deliver site-normalized turnover with sustained accessibility and recoverable mechanics across cycles are better positioned to translate nucleophilic depolymerization into scalable plastic upcycling [33,58].

The reported nearly quantitative PET or polyamide conversion rates often depend on the use of fine powders, excess nucleophiles, or short diffusion paths. These conditions inflate apparent activity but provide limited insight into scalable processes. Meaningful comparisons require strict controls such as site-normalized rates, polymer-to-reagent ratios, and durability testing using shaped specimens [59].

### *4.3. Photocatalytic and Oxidative Degradation*

In MOF-based photo-oxidative systems, light harvesting in the framework or in semiconductor heterojunctions generates charge carriers. These carriers form reactive oxygen species that cleave C–O and C–C bonds, while pore adsorption preorganizes chains and oligomers near sites that stabilize intermediates. A recent study by Ashaduzzaman et al. reported a MnOx/$TiO_2$@$NH_2$-ZIF-8 composite that achieved efficient removal of both cationic (MB) and anionic (DR81) dyes under sunlight by combining adsorption with photocatalysis [60]. The enhanced performance was attributed to band-gap tuning and improved charge-carrier separation within the heterojunction, consistent with ROS-mediated pathways that drive bond cleavage. Although this study was conducted in an aqueous dye system, the same design principles can be directly applied to light-driven polymer depolymerization. However, the actual reaction performance can be limited by several factors, such as polymer light scattering, restricted oxygen transport, and excessive product binding (overbinding), which may lead to a decrease in reaction rate. For this reason, evaluations should focus on external quantum efficiency, area-normalized space–time yield, product selectivity, and sustained activity on realistic mixed feeds rather than simple dye tests [6,7,14]. Figure 10 shows a VPOM–carbon nitride nanosheet heterostructure that proposes a Z-scheme pathway for acetate production. The evidence comes from spectroscopic signatures of superoxide and valence-band holes. Still, firm attribution requires several controls: full carbon accounting to confirm polymer-derived products, action spectra aligned with band edges, disclosure of peroxide additives, and checks for leaching or homogeneous Fenton-like chemistry. For durability, catalysts should also resist metal loss and nanoparticle outgrowth while maintaining porosity, wettability, and mechanical integrity after repeated cycles [33].

Platforms that combine efficient charge separation with accessible, fouling-resistant transport pathways are the most effective. When they also provide the above metrics under identical illumination and mass-transfer conditions, they are better positioned for scalable degradation and upcycling [15].

Many photocatalytic studies are performed with dyes or model substrates rather than real plastics, and often under unrealistic illumination conditions or with sacrificial oxidants. These conditions exaggerate efficiency and limit relevance to practical waste streams. Future efforts should focus on standardized action spectra, carbon balances, and long-term stability under mixed post-consumer plastics [8,11].

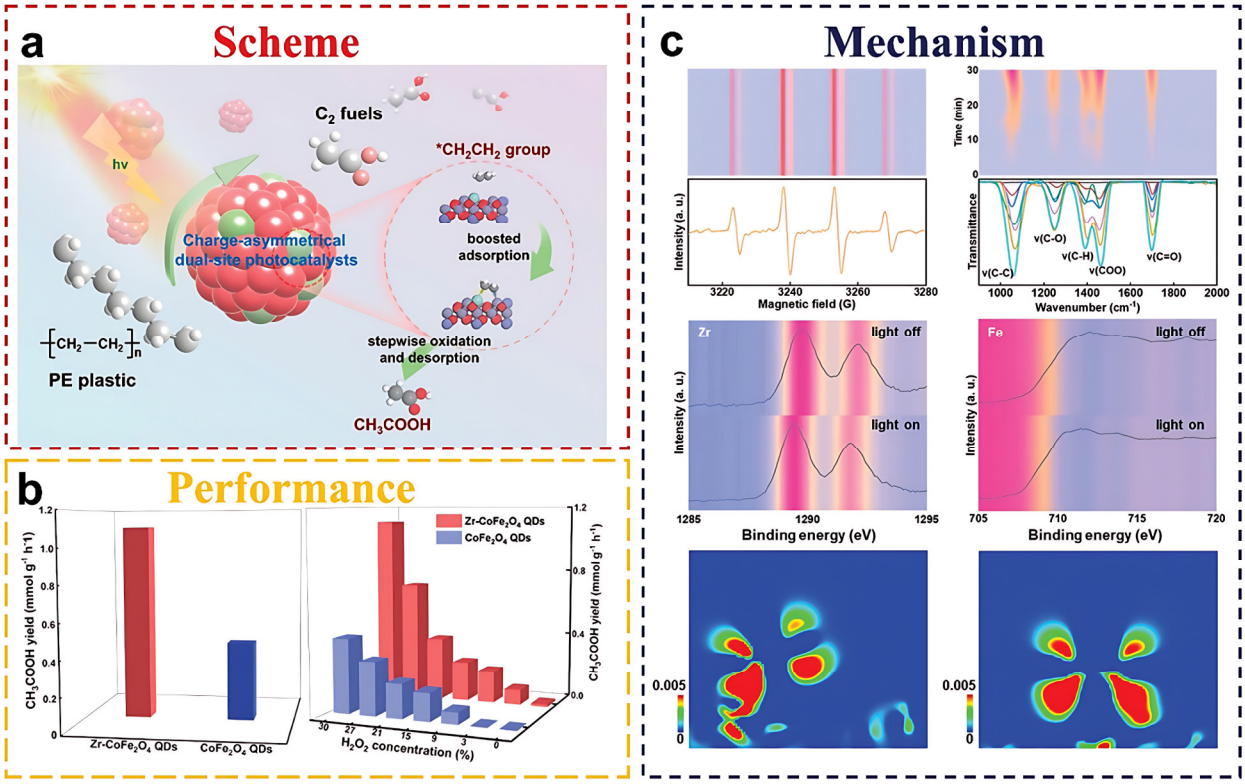



**Figure 10.** Photocatalytic conversion of plastics on VPOM and carbon nitride nanosheets. (**a**) Proposed Z-scheme charge separation and $CH_3COOH$ formation pathway from PE plastic. (**b**) Product yield comparison under various conditions. (**c**) ESR and XPS analyses confirming $O_2^{\bullet -}/h^+$ generation and Z-scheme charge transfer mechanism. Reproduced with permission from [16], Copyright 2025 American Chemical Society.

## 5. Depolymerization and Upcycling of Major Plastic Classes

### *5.1. Polyethylene Terephthalate (PET) Depolymerization*

Polyethylene terephthalate remains the workhorse polyester for packaging and textiles; however, its semi-crystalline morphology and strong ester bonds demand catalysts that couple carbonyl activation with effective transport of oligomers and products [61]. Zirconium- or hafnium-carboxylate frameworks and imidazolate frameworks have delivered high conversions and bis-hydroxyethyl terephthalate yields in batch glycolysis and hydrolysis, but performance in prior studies spans wide ranges of catalyst loading, ethylene-glycol-to-polymer ratio, temperature, and residence time, which makes direct comparison unreliable [62]. As summarized in Table 2 [63], prior studies often show 100 percent conversion with varying selectivity to bis-hydroxyethyl terephthalate; however, powder size, crystallinity of the feed, the presence of colorants and stabilizers, and external surface exposure frequently dominate outcomes.

Evidence for homogeneous contributions from dissolved metal species or linker fragments is rarely ruled out, so hot-filtration tests, leaching analysis, and site counts per accessible node are needed before assigning activity to framework sites. Meaningful benchmarking should therefore include site-normalized rates, space–time yield, monomer purity after isolation, polymer-to-reagent mass ratio, and activity retention with shaped bodies under repeated cycles. Platforms that maintain accessibility and durability in hot aqueous or alcoholic media while delivering high space–time yield are the most credible candidates for scalable PET upcycling. The standardized performance metrics used for benchmarking these MOF catalysts are summarized in Table S1 of the Supplementary Materials.

**Table 2.** PET depolymerization by MOF catalysts under different conditions, adapted with permission from [63]. Copyright © 2025 Elsevier.

| MOF | PET/Catalyst (w/w) | BHET (%) | PET Conversion (%) | Ethylene Glycol/PET (w/w) | Temperature (°C) | Time (h) | Pressure (atm) | References |
|---|---|---|---|---|---|---|---|---|
| MAF-6 | 100/1 | 81.7 | 92.4 | 6/1 | 180 | 4 | 1 | [64] |
| MAF-5 | 100/1 | 39 | 72.3 | 6/1 | 180 | 4 | 1 | |
| MAF-32 | 100/1 | 38.2 | 52.6 | 6/1 | 180 | 4 | 1 | |
| ZIF-8 | 100/1 | 73.6 | 100 | 5/1 | 190 | 1 | – | [31] |
| ZIF-67 | 100/1 | 79.5 | 100 | 5/1 | 190 | 1 | – | |
| ZIF-8/ZIF-67 | 100/1 | 83.4 | 100 | 5/1 | 190 | 1 | – | |
| ZIF-8 | 25/1 | 72.6 | 100 | 5/1 | 195 | 0.5 | 0.99 | [65] |
| DES@ ZIF-8 | 25/1 | 83.2 | 100 | 5/1 | 195 | 0.42 | 0.99 | |
| ZIF-8 | 100/1 | 76.75 | 100 | 5/1 | 197 | 1.5 | 1 | [62] |
| ZIF-67 | 100/1 | 76 | 100 | 5/1 | 197 | 2.5 | 1 | |
| MOF-5 | 100/1 | 73 | 100 | 5/1 | 197 | 3.5 | 1 | |
| ZIF-8 | 100/1 | 65.9 | 88.2 | 5/1 | 180 | 4 | 1 | [63] |
| DPZIF-8 | 100/1 | 76.1 | 91.7 | 5/1 | 180 | 4 | 1 | |

### *5.2. Polyurethane (PU) Chemical Recycling*

Polyurethane (PU) combines urethane linkages with phase-segregated hard and soft domains and a high fraction of additives, which together impede mass transport and complicate selective bond cleavage, so catalysts must couple carbonyl activation with pores and surfaces that admit swollen segments and allow rapid release [66]. Metal–organic frameworks with open metal sites can promote glycolysis and aminolysis by coordinating the carbamate carbonyl and delivering diols or amines within polar microenvironments; in many prior studies [19], headline conversions reflect large reagent-to-polymer ratios, fine powders, and short diffusion paths rather than intrinsic site productivity. Comparisons are meaningful only when rates are normalized to accessible sites and accompanied by space–time yield, polyol quality metrics such as hydroxyl number, acid and amine values, viscosity, and color, and refoam performance including compressive strength and cell morphology, alongside checks for metal leaching and retention of porosity in shaped bodies after multiple cycles.

Additive-rich streams can poison nodes or foul pores, and excessive defect creation or bulky grafts may raise apparent activity in small vials while reducing accessibility and mechanical integrity at scale. The most promising platforms pair Lewis acidity with wettable meso- or macropore pathways, maintain stability in hot glycols or amines, and demonstrate closed-loop value by converting recovered polyols into foams that meet specification [66], documented alongside solvent and energy use so that gains in upcycling are not offset by processing burdens.

### *5.3. Polyolefin (PE, PP) Bond Scission and Upcycling*

Polyethylene and polypropylene resist depolymerization because their backbones contain only C–C and C–H bonds, so effective upcycling hinges on catalysts that create reactive ensembles for hydrogenolysis or controlled oxidation while maintaining contact with semicrystalline solids; chain topology strongly influences accessibility and selectivity, with branching and crosslinking differences in LDPE, HDPE, LLDPE, PEX, and PP shaping adsorption and diffusion paths as summarized in Figure 11 [59,67]. In prior studies, single-site metals embedded in robust Zr- or Hf-based frameworks and MOF-derived metal–nitrogen–carbon motifs converted polyolefins to liquid hydrocarbons under lower severity

than thermal cracking [68]; however, performance often depended on high hydrogen pressure, swelling solvents, fine powders, and short diffusion lengths, which can obscure intrinsic site productivity.

Meaningful comparison requires site-normalized rates per accessible metal, carbon balances that distinguish polymer-derived products from solvent or catalyst, chain-length distributions and isomer ratios in the C4–C24 range, and stability of shaped bodies with retained porosity after cycling. Metal leaching, nanoparticle outgrowth, and pore collapse at elevated temperature remain common failure modes, and strong polymer binding can slow product release; interfacial engineering with wettable meso- or macropores and compatibilizers is therefore as important as maximizing gravimetric surface area. Systems that couple durable active sites with fouling-resistant transport and provide space–time yield, selectivity, and energy-use metrics on mixed post-consumer feeds are best positioned to translate polyolefin upcycling beyond laboratory vials [69].

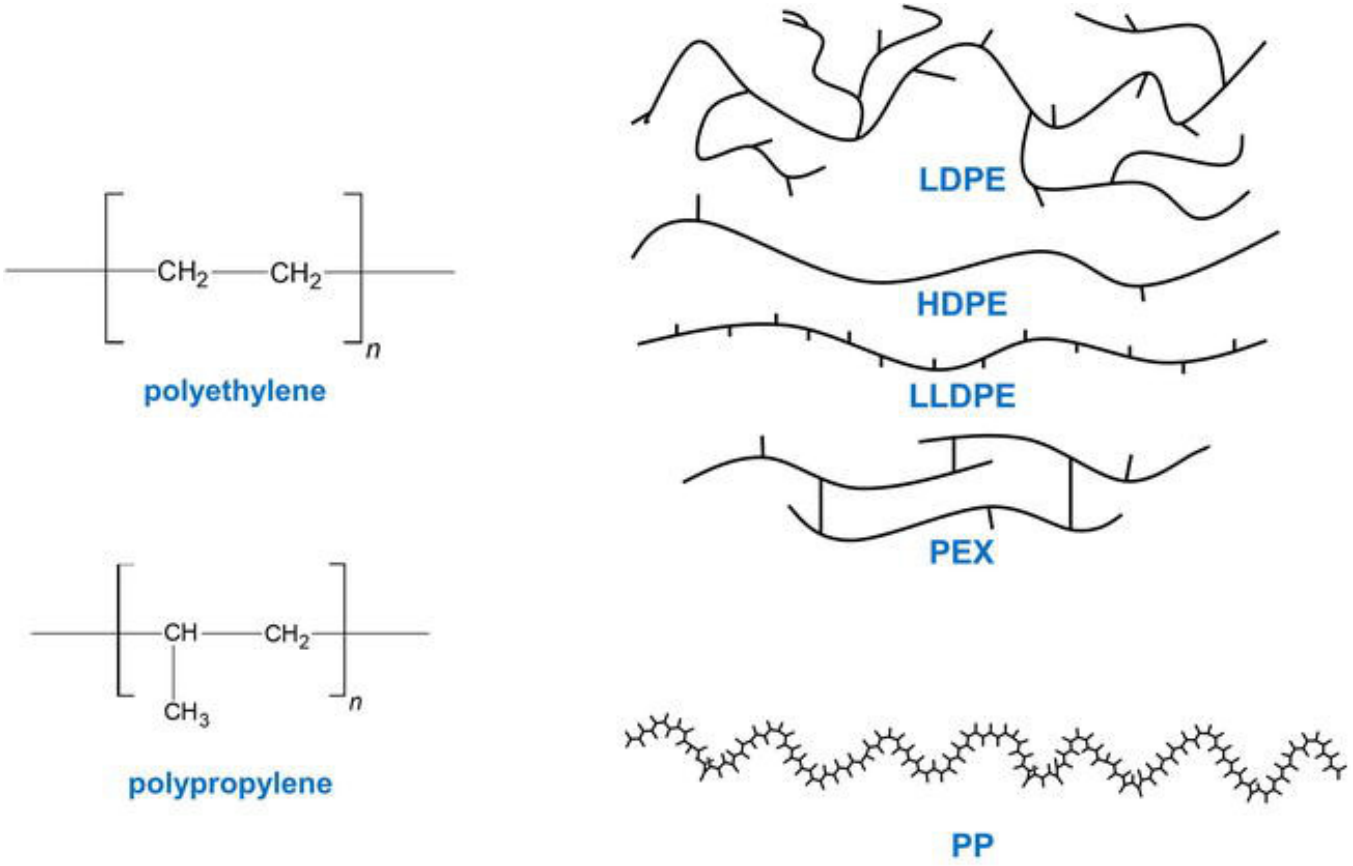



**Figure 11.** Chain architectures of polyethylene classes and polypropylene. Schematic repeat units of polyethylene and polypropylene with representative macromolecular topologies for LDPE, HDPE, LLDPE, and PEX, highlighting branching and crosslinking features that govern crystallinity, diffusion, and catalytic accessibility. Reprinted from [70], licensed under CC BY 3.0. © 2022 The Author(s), published by IntechOpen.

### *5.4. Polylactic Acid and Other Aliphatic Polyesters*

Polylactic acid dominates the market for biodegradable plastics [71]; however, true circularity requires routes that recover value with high selectivity and low severity rather than simple downcycling. Metal–organic frameworks with Lewis-acidic $Zr_6$ or $Hf_6$ nodes and MOF composites hosting Brønsted-acidic guests have enabled hydrolysis and alcoholysis of PLA to lactide, lactic acid, or alkyl lactates under comparatively mild conditions [72], although headline conversions in prior studies often reflect large alcohol-to-polymer ratios,

finely milled feeds, and short diffusion lengths that obscure intrinsic site productivity. Meaningful evaluation should include site-normalized rates, space–time yield, full carbon balance, and enantiomeric integrity since racemization during solvolysis can erode value. Additives and fillers common in consumer PLA depress apparent activity and complicate separations, while water activity and pore polarity steer the balance between backbiting to lactide and chain-end scission.

The same principles also extend to other aliphatic polyesters such as PBS, PBAT, PCL, and PGA [73], whose ester backbones are susceptible to nucleophilic attack, although mixed copolymer streams and aromatic comonomers in PBAT demand catalysts that discriminate among linkages or operate in tandem with selective adsorbents. Progress most likely to translate will pair durable acidity with wettable meso- or macropore access, demonstrate product purity suitable for repolymerization, and document the reuse of shaped bodies together with solvent and energy footprints so that gains in upcycling are not offset by processing burdens [29].

### *5.5. Toxicity and Environmental Impacts of Plastic Polymers*

Plastics remain in the environment for long periods not only because of their chemical stability and resistance to degradation, but also because they pose potential risks to ecosystems and human health. Polyethylene terephthalate (PET) is regarded as relatively stable, yet during degradation it can release antimony residues and organic dyes, which have been associated with cytotoxic responses and endocrine-disrupting effects [74,75]. Polyurethanes (PU) may break down into isocyanates and aromatic amines, substances linked to respiratory sensitization and possible carcinogenicity [76,77]. Although polyolefins (PE and PP) are largely chemically inert, their fragmentation into micro- and nanoplastics leads to physical accumulation in organisms, increased adsorption of persistent organic pollutants, and inflammatory reactions [78,79]. Polylactide (PLA) and other bioplastics are often marketed as "biodegradable," but under natural conditions, their degradation is frequently incomplete, releasing microplastic particles and lactic acid oligomers that can disturb microbial populations and alter the pH of aquatic systems [80,81]. In summary, the hazards associated with plastics stem from both their degradation by-products and the chemical additives introduced during production, underscoring the need for MOF-based depolymerization approaches that minimize harmful secondary effects.

## 6. Reactor Engineering and Process Integration for MOF-Catalyzed Plastic Degradation and Upcycling

### *6.1. Batch Versus Continuous-Flow Configurations*

Batch autoclaves remain effective for discovery and for producing highly crystalline MOFs, but their scale is constrained by long residence times, heavy solvent use, and limited control over mixing and heat removal [82]. Continuous-flow reactors lift space–time yield through rapid heating and controlled supersaturation, although fouling, corrosion, and heat transfer gradients can compromise quality and uptime if not engineered. In the case of MOF-808, minute-scale residence times were found to achieve batch-level crystallinity [83], with PXRD patterns consistently maintained from 1 to 120 min. TEM observations revealed uniform microcrystalline particles, distinct from the larger crystallites typically obtained under batch conditions.

These advantages are meaningful only when productivity is considered alongside particle size distribution, defect density, residual modulator content, filterability, and post-reaction robustness, as overly aggressive nucleation can artificially enhance apparent activity while compromising hydrolytic stability and mechanical strength in shaped bodies. Table 3 compiles representative continuous-flow syntheses across microflow, packed-bed,

and column formats, underscoring the diversity of reactor options but also the need for common metrics such as site-normalized rates, space–time yield with solvent and energy footprints, and retention of porosity and crush strength after cycling. Manufacturing routes that couple high throughput with controlled defect populations, reproducible morphology, and compatibility with pelletization or monolith formation are the ones most likely to translate to durable MOF catalysts for plastic depolymerization and upcycling [84].

**Table 3.** Representative MOFs obtained in a continuous-flow reactor, adapted with permission from [85]. Copyright © 2024 Wiley-VCH GmbH.

| Catalyst | Reactor Type | Reaction Type | Activity | Stability | Reference |
|---|---|---|---|---|---|
| Ni@C-300R | fixed-bed continuous down-flow quartz reactor | Semi-hydrogenation of phenylacetylene to styrene | 99.3 % PA conversion and 92.0 % ST selectivity[a] | stable for 5 h | [86] |
| Pd/UiO-66(Hf) | liquid-phase continuous down-flow quartz reactor | Semi-hydrogenation of phenylacetylene to styrene | 99 % PA conversion and 90 % ST selectivity[a] | Reused 4 times | [87] |
| PCN-160-Pd | microflow | Suzuki–Miyaura coupling | TON of 18 for 12 h | NA | [88] |
| CuBTC[b] | stainless-steel column packed | Intramolecular condensation reaction for the synthesis of xanthene derivatives | yield of 33 % ± 14 % | NA | [89] |
| MIL-100(Sc)@PBSAC[c] | packed-bed reactors | Intramolecular cyclization of (±)-citronellal | Selectivity to 88.8 ± 6.5 | NA | [90] |
| MIL-100(Fe) | microreactor | Acetalization of aldehyde | Conversion over 90 % for more than 96 h | NA | [91] |

### *6.2. Fixed-Bed and Membrane Reactors with Immobilized MOFs*

Translating MOF catalysis to continuous operation requires immobilization strategies that preserve activity and porosity while delivering mechanical strength and low pressure drop [92]. Fixed-bed formats based on pellets, monoliths, or coated packings provide straightforward reactor integration and enable control of residence time and space–time yield, although binders, supports, and growth methods must be chosen to avoid pore blockage, metal leaching, or attrition under solvent flow, oxidants, and thermal cycling. Prior studies with enzyme–MOF hybrids [93] and MOF–carbon composites [90] demonstrate multi-cycle stability in flow, which underscores the promise of cooperative microenvironments, but performance should always be benchmarked with site-normalized rates, breakthrough curves, and post-run crush strength together with analyses of fouling and deactivation.

Membrane reactors extend this concept by using MOF layers as reactive interfaces that couple selective transport with catalysis [94], offering in situ removal of products or water to shift equilibria; their relevance to plastic depolymerization depends on sustained flux, selectivity under complex feeds, chemical compatibility with glycols or oxidants, and regeneration protocols that restore permeability without damaging the framework. For microplastic streams, immobilization prevents catalyst loss and aggregation while allowing continuous hydrolysis, alcoholysis, or oxidation, provided that mass-transfer

limitations across swollen polymer layers are mitigated through hierarchical porosity and wettable macrochannels. The most credible reactor architectures pair robust shaping and defect control with metrics that matter at scale, including pressure drop, weight-hourly space velocity, flux per membrane area, leaching and particle-size stability, and activity retention over many cycles, so that catalytic gains translate into durable operation for plastic depolymerization and upcycling.

### 6.3. Coupling MOF Catalysis with Enzymatic or Electrochemical Steps

Coupling MOF catalysis with biocatalysts or electrochemical steps creates hybrid platforms that merge molecular precision with reactor control, where open metal sites preorganize substrates and generate intermediates that enzymes or electrogenerated species transform with selectivity [52,53]. Enzyme–MOF assemblies can stabilize fragile hydrolases and oxidases in hot aqueous or alcoholic media and can stage cascades in which a MOF first activates ester or C–C bonds and an immobilized enzyme completes depolymerization or channels products toward targeted monomers; however, benefits fade when pores are blocked by proteins or polymers, when cofactors are depleted, or when local pH swings and oxidants deactivate the enzyme, so designs should quantify enzyme loading, effective diffusivity of oligomers, turnover per active protein, and activity retention after many cycles.

Electrochemical coupling offers in situ generation of nucleophiles, redox equivalents, or hydrogen peroxide and superoxide at MOF interfaces and on conductive MOF composites, enabling selective oxidation, reductive hydrogenolysis, or localized pH control that shortens pathways to valuable oxygenates, but low intrinsic conductivity, metal leaching, and homogeneous Fenton chemistry can dominate if supports and potentials are not tuned [95–97]. Prior studies have demonstrated progress with redox linkers, carbon composites, and MOF-derived M–N–C electrodes; however, meaningful comparisons require the evaluation of current density, faradaic efficiency, energy intensity, carbon balance, and stability of shaped electrodes with preserved porosity and crush strength. Hybrid systems that maintain enzyme integrity, suppress leaching, and deliver site-normalized rates together with high space–time yield on mixed post-consumer feeds are best positioned to convert MOF catalysis from promising vials to robust continuous processes for plastic depolymerization and upcycling.

## 7. System-Level Assessment for MOF-Enabled Plastic Recycling

### 7.1. Life Cycle Assessment and Deployment Metrics

Evaluating MOFs for plastic depolymerization and upcycling requires environmental accounting that encompasses performance from synthesis to end of life, rather than performance metrics in isolation. Life cycle assessment provides this accounting when the functional unit, system boundaries, solvent recovery, electricity mix, and yield assumptions are stated, and when results are given both per kilogram of MOF and per unit of catalytic service, such as kilograms of plastic converted. Prior studies have shown that solvent choice and synthesis route have a significant impact on many frameworks, with extrusion or other solvent-minimal routes substantially reducing carcinogenicity, global warming potential, eutrophication, and ecotoxicity relative to DMF-based solvothermal synthesis [98] as summarized in Figure 12 [99]. These gains are meaningful only if crystallite size distribution, defect density, residual salts, filterability, and drying energy are disclosed and if durability in shaped bodies is demonstrated so that the footprint is amortized over many cycles.

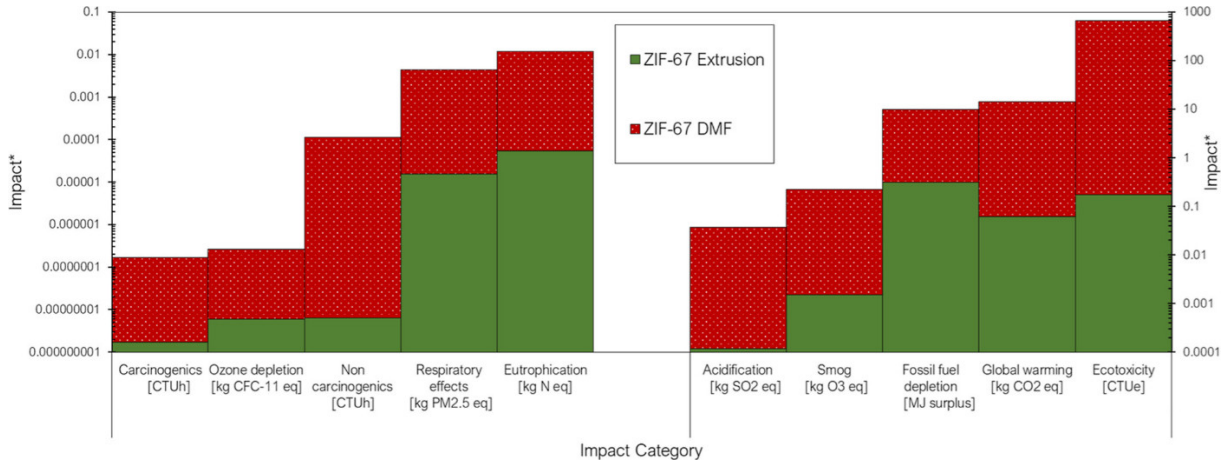



**Figure 12.** Life cycle impacts for ZIF-67 synthesis. Comparison of extrusion and DMF solvothermal routes across representative TRACI categories showing consistently lower burdens for extrusion, highlighting the influence of solvent choice and synthesis route on the environmental profile of MOFs. * Impact values are normalized dimensionless scores based on TRACI midpoint indicators. Reprinted from [99], licensed under CC BY 4.0. © 2017 The Author(s), published by Elsevier.

For catalytic deployment, the relevant metrics include net greenhouse gas balance per kilogram of plastic treated after displacement credits for recovered monomers, solvent and water use per kilogram of product, energy intensity, leaching and waste neutralization, and retention of porosity and crush strength after cycling. Comparative claims should therefore pair space–time yield and selectivity with cradle to gate and use phase impacts, and should report break-even cycle counts that show how many runs are required before the catalyst becomes carbon positive. Platforms that combine low-impact manufacturing, high durability in working media, and transparent accounting of avoided virgin production are the ones most likely to deliver credible environmental gains alongside chemical performance.

### *7.2. Techno-Economic Benchmarking of MOF-Enabled Recycling Pathways*

A fair comparison with incumbent recycling must couple performance with cost and scale metrics, rather than relying solely on laboratory conversions. Mechanical reprocessing remains the most cost-effective option when clean, single-polymer streams are available, while pyrolysis favors mixed polyolefins but produces broad product slates that require upgrading [100]. MOF-enabled solvolysis and hydrogenolysis promise higher selectivity at lower severity and can deliver polymerization-grade monomers or tailored intermediates, although viability hinges on space–time yield, solvent or hydrogen make-up, and catalyst lifetime in shaped bodies. Prior studies indicate that aqueous or solvent-minimal manufacture can push catalyst prices toward the tens of dollars per kilogram, but economic advantage only materializes when site-normalized rates are high enough to amortize catalyst and shaping costs, when solvent recovery exceeds large fractions, and when durability is demonstrated over many cycles without loss of porosity or crush strength.

Claims of circular value should therefore be framed with a consistent functional unit, such as kilograms of plastic converted, and accompanied by the minimum product selling price, carbon and energy balances, reagent-to-polymer ratios, monomer purity after isolation, and downtime from fouling or leaching. Using plastic-derived linkers or MOF–polymer composites may reduce precursor costs or enable process integration [8], although the benefits depend on purification burdens and whether the composite improves flux, selectivity, or catalyst retention in flow. The most credible opportunities are those where MOFs shorten separations, increase selectivity to high-value products, operate in continuous reactors with low pressure drop, and maintain activity in real feeds contain-

ing dyes, fillers, stabilizers, and moisture, thereby aligning techno-economic gains with environmental performance [9].

### *7.3. Catalyst Regeneration, Stability, and Leaching Control*

Translating MOF catalysts to continuous plastic degradation demands evidence that active sites, pore connectivity, and mechanical strength persist through realistic cycling in hot water, alcohols, and oxidants while metals remain immobilized within the framework [101]. Prior studies with robust Zr and Hf carboxylates have shown promising reuse, although increases in defect density, linker hydrolysis, or binder interactions during shaping can lower accessibility and weaken pellets or monoliths even when initial conversions are high. A rigorous program should quantify site-normalized activity retention, crush strength, and attrition loss, as well as pressure drop and porosity before and after operation, together with ICP-based metal balances on feeds and effluents to rule out homogeneous pathways [102].

Controls such as hot filtration, chelating scavengers, and three-phase tests help distinguish framework-bound turnover from contributions of dissolved species or exsolved nanoparticles, a risk that grows under photo or electrochemical conditions where linkers can oxidize and nodes can transform. Regeneration protocols need to remove fouling without damaging the lattice, which favors solvent rinses, mild oxidative cleans, modulator-assisted defect healing, and ligand exchange that restore node coordination rather than aggressive calcination that collapses pores [103]. Additives and dyes in real streams can poison Lewis-acidic nodes or foul mesopores, so adsorption coefficients for relevant oligomers, leaching rates, and recovery of permeability and activity after regeneration should accompany conversion data. Platforms most likely to advance are those that pair hydrolytic endurance with healable defect chemistry, preserve transport in shaped bodies, and demonstrate low leaching across multiple cycles so that catalyst replacement and waste treatment costs do not erase the gains from efficient depolymerization and upcycling.

Given these limitations, it is essential to benchmark MOF catalysts using standardized performance metrics. Table 4 summarizes representative studies across different polymers in terms of space–time yield (STY), selectivity, and product purity. Although complete datasets are not always reported, even partial comparisons highlight the importance of standardized reporting to enable meaningful benchmarking across different systems.

**Table 4.** Representative MOF-based studies for plastic depolymerization and upcycling, summarized by standardized performance metrics.

| Polymer | MOF Catalyst | Reaction Conditions | STY ($kg \cdot m^{-3} \cdot day^{-1}$) | Selectivity (%) | Product Purity (%) | Reference |
|---|---|---|---|---|---|---|
| PET | UiO-66-$NH_2$ | 180 °C, EG solvent, 24 h | ~0.45 | 85 | 92 (BHET) | [64,65,104] |
| PET | MOF-808 | 150 °C, aqueous, 12 h | 0.32 | 78 | 88 (TPA) | [64,65,104] |
| PU | Zn-MOF | 120 °C, methanol, 10 h | 0.20 | 70 | - | [62,66] |
| PE/PP | MIL-101(Fe) | Photocatalysis, 300 W Xe lamp | - | 65 | 80 (oxidized frag) | [69–71] |
| PLA | Zr-MOF (MIP-202) | Hydrolytic, 90 °C, water | 0.15 | 82 | 95 (lactic acid) | [29] |

## 8. Challenges and Future Opportunities

### *8.1. Limitations and Challenges*

Practical deployment depends on MOFs that keep active sites accessible and transport pathways open in humid, salty, and organic-rich media while retaining strength in pellets or monoliths [27,28,105,106]. Water dissociation at nodes, competitive adsorption by natural organic matter, and exposure to bases or oxidants can cap sites, erode crystallinity, and raise pressure drop [107,108]. Promising countermeasures include hydrophobic ligand substitution, high-valent nodes, defect healing, and core–shell architectures that slow ingress of deactivating species, although these same edits can narrow necks and lengthen diffusion paths [43,109]. Credible durability, therefore, pairs site-normalized activity retention in buffered water or alcohols with post-cycle porosity, crystallinity, crush strength, and leaching mass balances, plus regeneration protocols that restore permeability without damaging the lattice [110]. Single-atom motifs and defect engineering expand the palette of catalytic ensembles and can sharpen polarity, redox character, and adsorption strength around targeted nodes [111,112], although the added reactivity can come with mechanical weakening, broadened pore distributions, microstrain, and a higher risk of nanoparticle growth or metal loss in hot liquids [113]. Assertions of isolated-site turnover warrant quantitative site counts, hot-filtration and scavenger controls, and operando probes that track the node–linker environment under working media [114].

Comparisons are meaningful only when normalized to accessible sites and accompanied by adsorption coefficients for relevant oligomers, monomer purity after isolation, and retention of porosity and crush strength after regeneration, with hierarchical porosity and healable defect chemistry used to balance accessibility with robustness [115,116]. Photo, electro, and bio hybrid platforms create lower-severity routes to selective scission and targeted upgrading through reactive oxygen species, electro-generated reductants and oxidants, or stabilized hydrolases [117–120]. Their value rests on metrics that matter at scale, including external quantum efficiency, faradaic efficiency, energy intensity, and carbon accounting that confirms polymer-derived products, together with the stability of electrodes, membranes, or pellets under realistic flows and mixed post-consumer feeds containing dyes, fillers, and stabilizers [120,121].

Platforms that maintain accessibility and mechanics while delivering high space–time yield under matched mass-transfer limits, and that are documented with transparent life-cycle and techno-economic metrics, are best positioned to move MOF catalysis from promising vials to dependable processes for plastic depolymerization and upcycling [122,123].

### *8.2. Future Opportunities*

The future of MOF-based plastic depolymerization lies in the convergence of materials design, process intensification, and digital optimization. Emerging synthesis routes such as continuous-flow, mechanochemical, and solvent-free processes are reducing the cost and environmental burden of large-scale MOF fabrication [124,125]. These scalable routes also enhance batch reproducibility and facilitate shaping MOFs into monoliths or membranes with improved mechanical integrity. Hybrid catalytic architectures that integrate MOFs with enzymes, photocatalysts, or redox mediators represent a promising frontier for selective polymer bond scission under mild conditions [15,126,127]. For instance, photo-electrocatalytic MOF systems enable simultaneous oxidation and reduction reactions, lowering the energy input and generating high-purity monomers from mixed plastic waste streams. Similarly, the incorporation of defect healing and hierarchical porosity offers a tunable balance between reactivity and stability, extending catalyst lifetimes under humid or oxidizing environments. Beyond laboratory performance, standardized performance metrics, including space–time yield (STY), selectivity, and product purity, will play a crucial

role in benchmarking catalytic efficiency and facilitating machine-learning-based discovery of next-generation MOFs [128]. Integrating such metrics with life-cycle assessment (LCA) and techno-economic analysis (TEA) will provide a holistic understanding of environmental and industrial viability. Finally, coupling MOF catalysis with renewable energy-driven processes, such as solar, photoelectrochemical, or bio-assisted depolymerization, is expected to redefine sustainable polymer recycling. Through these multidisciplinary strategies, MOF-based platforms could evolve from conceptual frameworks to scalable technologies that enable circular plastic economies and environmentally responsible upcycling [129].

## 9. Conclusions

MOF-enabled plastic degradation and upcycling will advance most rapidly where catalytic function is combined with transport and form factors. Nucleophilic scission benefits from Lewis-acidic nodes and wettable hierarchical pores, but performance must be normalized to accessible sites and sustained under working media rather than inferred from high-surface-area powders. Reactor choices matter as much as chemistry, since continuous-flow synthesis and processing can deliver minute-scale residence times at batch-level crystallinity only when defect populations, particle-size distributions, modulator residues, and post-reaction robustness are controlled and disclosed. Credible deployment likewise requires shaped bodies and membranes that retain porosity, crush strength, particle size, and low pressure drop under cycling, with leaching and stability tracked so that activity gains translate into durable operation. Environmental and economic accounting must travel with performance from synthesis to the end of life. Solvent-minimal manufacturing can lower impacts across multiple categories relative to conventional solvothermal routes, but such gains matter only when crystallite quality, residual salts, drying energy, and durability in shaped bodies are documented and amortized over many cycles. Techno-economic benchmarking indicates that MOF-enabled solvolysis or hydrogenolysis can outperform incumbents in terms of selectivity at lower severity, provided that site-normalized rates, solvent or hydrogen make-up, and long-lived catalysts push costs toward practical targets. These results are reported with consistent functional units alongside downtime, purity, and energy balances. The most credible opportunities combine low-impact manufacturing, high durability in working media, transparent accounting of avoided virgin production, and high space–time yield, aligning environmental gains with chemical performance.

In conclusion, MOFs have shown significant promise for the selective depolymerization and upcycling of plastics. However, further progress requires standardized metrics, scalable engineering solutions, and integration with life-cycle and techno-economic analyses. More importantly, this review goes beyond factual synthesis. It emphasizes the adoption of unified performance benchmarks such as space–time yield, selectivity, and product purity. It also highlights the engineering requirements for scale-up, including packed-bed and continuous-flow operation, and explicitly connects MOF catalysis to environmental and techno-economic assessments. By reinforcing these distinctive perspectives, we aim to provide a comparative and application-oriented framework that can guide both academic research and industrial translation in the years ahead.

**Supplementary Materials:** The following supporting information can be downloaded at: https://www.mdpi.com/article/10.3390/cryst15100897/s1. Table S1: Standardized performance metrics for MOF-enabled plastic depolymerization and upcycling.

**Author Contributions:** Conceptualization, H.-O.K. and M.K.; methodology, K.L., S.H. and K.S.L.; software, B.-s.K.; validation, M.K. and S.-J.H.; formal analysis, K.L. and S.H.; investigation, K.L., M.K. and B.-s.K.; resources, J.-A.P. and S.-J.H.; data curation, M.K. and B.-s.K.; writing—original draft preparation, K.L. and S.H.; writing—review and editing, H.-O.K., M.K. and B.-s.K.; visualization,

K.L. and S.H.; supervision, H.-O.K.; project administration, K.S.L. and J.-A.P.; funding acquisition, H.-O.K., K.S.L., S.-J.H. and J.-A.P. All authors have read and agreed to the published version of the manuscript.

**Funding:** This work was supported by a grant from the National Research Foundation of Korea, funded by the Korean government through the Korea Institute of Planning (RS-2025-00512586), this work was supported by a Korea Foundation for Women In Science, Engineering and Technology (WISET) grant, funded by the Ministry of Science and ICT (MSIT) under the Team (WISET-2025-112) Research Program for female engineering students and this research was supported by the Regional Innovation System & Education (RISE) Glocal University 30 Project program, funded by the Ministry of Education (MOE) and the Gangwon State (G.S.), Republic of Korea (2025-RISE-10-002).

**Data Availability Statement:** No new data were generated or analyzed in this study. All data supporting the statements in this review are available in the cited literature.

**Conflicts of Interest:** The authors declare no conflicts of interest.

## Abbreviations

The following abbreviations are used in this manuscript:

| | |
|---|---|
| MOF | Metal–Organic Framework |
| COF | Covalent Organic Framework |
| ZIF | Zeolitic Imidazolate Framework |
| PET | Poly(ethylene terephthalate) |
| BHET | Bis(hydroxyethyl) terephthalate |
| PU | Polyurethane |
| PE | Polyethylene |
| PP | Polypropylene |
| PLA | Polylactic Acid |
| PBS | Poly(butylene succinate) |
| PBAT | Poly(butylene adipate-co-terephthalate) |
| PCL | Poly(ε-caprolactone) |
| PGA | Polyglycolic Acid |
| PA | Phenylacetylene |
| ST | Styrene |
| TRACI | Tool for the Reduction and Assessment of Chemical and Other Environmental Impacts |

## References

1. Shah, H.H.; Amin, M.; Iqbal, A.; Nadeem, I.; Kalin, M.; Soomar, A.M.; Galal, A.M. A review on gasification and pyrolysis of waste plastics. *Front. Chem.* **2023**, *10*, 960894. [CrossRef]
2. Lopez, G.; Artetxe, M.; Amutio, M.; Alvarez, J.; Bilbao, J.; Olazar, M. Recent advances in the gasification of waste plastics. A critical overview. *Renew. Sustain. Energy Rev.* **2018**, *82*, 576–596. [CrossRef]
3. Geyer, R.; Jambeck, J.R.; Law, K.L. Production, use, and fate of all plastics ever made. *Sci. Adv.* **2017**, *3*, e1700782. [CrossRef] [PubMed]
4. Andrady, A.L. Microplastics in the marine environment. *Mar. Pollut. Bull.* **2011**, *62*, 1596–1605. [CrossRef] [PubMed]
5. Jehanno, C.; Alty, J.W.; Roosen, M.; De Meester, S.; Dove, A.P.; Chen, E.Y.-X.; Leibfarth, F.A.; Sardon, H. Critical advances and future opportunities in upcycling commodity polymers. *Nature* **2022**, *603*, 803–814. [CrossRef]
6. Li, J.-R.; Kuppler, R.J.; Zhou, H.-C. Selective gas adsorption and separation in metal–organic frameworks. *Chem. Soc. Rev.* **2009**, *38*, 1477–1504. [CrossRef]
7. Weng, Y.; Hong, C.-B.; Zhang, Y.; Liu, H. Catalytic depolymerization of polyester plastics toward closed-loop recycling and upcycling. *Green Chem.* **2024**, *26*, 571–592. [CrossRef]
8. Wu, P.; Guo, M.; Zhang, R.W.; Huang, Q.; Wang, G.; Lan, Y.Q. When microplastics/plastics meet metal-organic frameworks: Turning threats into opportunities. *Chem. Sci.* **2024**, *15*, 17781–17798. [CrossRef]
9. Nguyen, B.T.; Tan, T.T.Y.; Otake, K.I.; Kitagawa, S.; Lim, J.Y.C. MOF Catalysts for Plastic Depolymerization. *Angew. Chem. Int. Ed.* **2025**, *64*, e202504017. [CrossRef]

10. Slater, B.; Wong, S.O.; Duckworth, A.; White, A.J.P.; Hill, M.R.; Ladewig, B.P. Upcycling a plastic cup: One-pot synthesis of lactate containing metal organic frameworks from polylactic acid. *Chem. Commun.* **2019**, *55*, 7319–7322. [CrossRef]
11. Yaghi, O.M. Reticular Chemistry—Construction, Properties, and Precision Reactions of Frameworks. *J. Am. Chem. Soc.* **2016**, *138*, 15507–15509. [CrossRef] [PubMed]
12. Nikhar, S.; Kumar, P.; Chakraborty, M. A review on microplastics degradation with MOF: Mechanism and action. *Next Nanotechnol.* **2024**, *5*, 100060. [CrossRef]
13. Yun, L.-X.; Qiao, M.; Zhang, B.; Zhang, H.-T.; Wang, J.-X. Upcycling plastic wastes into high-performance nano-MOFs by efficient neutral hydrolysis for water adsorption and photocatalysis. *J. Mater. Chem. A* **2024**, *12*, 19452–19461. [CrossRef]
14. Wang, S.; Wang, X. Multifunctional metal–organic frameworks for photocatalysis. *Small* **2015**, *11*, 3097–3112. [CrossRef]
15. Zhang, T.; Lin, W. Metal–organic frameworks for artificial photosynthesis and photocatalysis. *Chem. Soc. Rev.* **2014**, *43*, 5982–5993. [CrossRef]
16. Wan, Y.; Wang, H.; Huo, P. Plastic Degradation and Conversion by Photocatalysis. In *Plastic Degradation and Conversion by Photocatalysis (Volume 2): From Waste to Wealth*; American Chemical Society Publications: Washington, DC, USA, 2024; pp. 1–22.
17. Xiao, C.; Tian, J.; Chen, Q.; Hong, M. Water-stable metal-organic frameworks (MOFs): Rational construction and carbon dioxide capture. *Chem. Sci.* **2024**, *15*, 1570–1610. [CrossRef]
18. Clark, R.A.; Shaver, M.P. Depolymerization within a Circular Plastics System. *Chem. Rev.* **2024**, *124*, 2617–2650. [CrossRef]
19. Mastropietro, T.F. Metal-organic frameworks and plastic: An emerging synergic partnership. *Sci. Technol. Adv. Mater.* **2023**, *24*, 2189890. [CrossRef]
20. Larrain, M.; Van Passel, S.; Thomassen, G.; Van Gorp, B.; Nhu, T.T.; Huysveld, S.; Van Geem, K.M.; De Meester, S.; Billen, P. Techno-economic assessment of mechanical recycling of challenging post-consumer plastic packaging waste. *Resour. Conserv. Recycl.* **2021**, *170*, 105607. [CrossRef]
21. du Preez, W.; Mauchline, D.A.; van der Merwe, A.F.; van der Walt, J.; Becker, T.; Modiba, R.; Chauke, H.; Dzogbewu, T.; Mostert, R.; Maringa, M.; et al. Review of the current state-of-the-art in plasma gasification of municipal and medical waste. *MATEC Web Conf.* **2024**, *406*, 05008.
22. Yin, Y.; Zhang, Y.; Zhou, X.; Gui, B.; Wang, W.; Jiang, W.; Zhang, Y.-B.; Sun, J.; Wang, C. Ultrahigh–surface area covalent organic frameworks for methane adsorption. *Science* **2024**, *386*, 693–696. [CrossRef]
23. Chen, Z.; Hanna, S.L.; Redfern, L.R.; Alezi, D.; Islamoglu, T.; Farha, O.K. Reticular chemistry in the rational synthesis of functional zirconium cluster-based MOFs. *Coord. Chem. Rev.* **2019**, *386*, 32–49. [CrossRef]
24. Wang, L.; Qiao, W.; Liu, H.; Li, S.; Wu, J.; Hou, H. Synergistic Effects of Lewis Acid-Base Pair Sites—Hf-MOFs with Functional Groups as Distinguished Catalysts for the Cycloaddition of Epoxides with $CO_2$. *Inorg. Chem.* **2023**, *62*, 3817–3826. [CrossRef] [PubMed]
25. Wu, Y.; Wang, X.; Kirlikovali, K.O.; Gong, X.; Atilgan, A.; Ma, K.; Schweitzer, N.M.; Gianneschi, N.C.; Li, Z.; Zhang, X.; et al. Catalytic Degradation of Polyethylene Terephthalate Using a Phase-Transitional Zirconium-Based Metal-Organic Framework. *Angew. Chem. Int. Ed.* **2022**, *61*, e202117528.
26. Vandenhaute, S.; Cools-Ceuppens, M.; DeKeyser, S.; Verstraelen, T.; Van Speybroeck, V. Machine learning potentials for metal-organic frameworks using an incremental learning approach. *npj Comput. Mater.* **2023**, *9*, 19. [CrossRef]
27. Kim, J.Y.; Kang, J.; Cha, S.; Kim, H.; Kim, D.; Kang, H.; Choi, I.; Kim, M. Stability of Zr-Based UiO-66 Metal-Organic Frameworks in Basic Solutions. *Nanomaterials* **2024**, *14*, 110. [CrossRef]
28. Zuluaga, S.; Fuentes-Fernandez, E.M.A.; Tan, K.; Xu, F.; Li, J.; Chabal, Y.J.; Thonhauser, T. Understanding and controlling water stability of MOF-74. *J. Mater. Chem. A* **2016**, *4*, 5176–5183. [CrossRef]
29. Li, Y.; Wang, S.; Qian, S.; Liu, Z.; Weng, Y.; Zhang, Y. Depolymerization and re/upcycling of biodegradable PLA plastics. *ACS Omega* **2024**, *9*, 13509–13521. [CrossRef]
30. Fan, D.; Naskar, S.; Maurin, G. Unconventional mechanical and thermal behaviours of MOF CALF-20. *Nat. Commun.* **2024**, *15*, 3251. [CrossRef]
31. Wang, T.; Shen, C.; Yu, G.; Chen, X. Fabrication of magnetic bimetallic Co–Zn based zeolitic imidazolate frameworks composites as catalyst of glycolysis of mixed plastic. *Fuel* **2021**, *304*, 121397. [CrossRef]
32. Wang, S.-Q.; Gu, X.; Wang, X.; Zhang, X.-Y.; Dao, X.-Y.; Cheng, X.-M.; Ma, J.; Sun, W.-Y. Defect-engineering of Zr (IV)-based metal-organic frameworks for regulating $CO_2$ photoreduction. *Chem. Eng. J.* **2022**, *429*, 132157. [CrossRef]
33. Sun, J.; Dong, J.; Gao, L.; Zhao, Y.-Q.; Moon, H.; Scott, S.L. Catalytic upcycling of polyolefins. *Chem. Rev.* **2024**, *124*, 9457–9579. [CrossRef]
34. Garzon-Tovar, L.; Carné-Sánchez, A.; Carbonell, C.; Imaz, I.; Maspoch, D. Optimised room temperature, water-based synthesis of CPO-27-M metal–organic frameworks with high space-time yields. *J. Mater. Chem. A* **2015**, *3*, 20819–20826. [CrossRef]
35. Shearer, G.C.; Chavan, S.; Bordiga, S.; Svelle, S.; Olsbye, U.; Lillerud, K.P. Defect engineering: Tuning the porosity and composition of the metal–organic framework UiO-66 via modulated synthesis. *Chem. Mater.* **2016**, *28*, 3749–3761. [CrossRef]

36. Burtch, N.C.; Jasuja, H.; Walton, K.S. Water stability and adsorption in metal–organic frameworks. *Chem. Rev.* **2014**, *114*, 10575–10612. [CrossRef] [PubMed]
37. Vermoortele, F.; Bueken, B.; Le Bars, G.; Van de Voorde, B.; Vandichel, M.; Houthoofd, K.; Vimont, A.; Daturi, M.; Waroquier, M.; Van Speybroeck, V. Synthesis modulation as a tool to increase the catalytic activity of metal–organic frameworks: The unique case of UiO-66 (Zr). *J. Am. Chem. Soc.* **2013**, *135*, 11465–11468. [CrossRef] [PubMed]
38. Raja, D.S.; Tsai, D.-H. Recent advances in continuous flow synthesis of metal–organic frameworks and their composites. *Chem. Commun.* **2024**, *60*, 8497–8515. [CrossRef]
39. Friščić, T.; Mottillo, C.; Titi, H.M. Mechanochemistry for synthesis. *Angew. Chem.* **2020**, *132*, 1030–1041. [CrossRef]
40. Trickett, C.A.; Gagnon, K.J.; Lee, S.; Gándara, F.; Bürgi, H.B.; Yaghi, O.M. Definitive molecular level characterization of defects in UiO-66 crystals. *Angew. Chem. Int. Ed.* **2015**, *54*, 11162–11167. [CrossRef]
41. Pereira, D.; Sardo, M.; Vieira, R.; Marín-Montesinos, I.; Mafra, L. Enhancing $CO_2$ Capture Via Fast Microwave-Assisted Synthesis of the CALF-20 Metal–Organic Framework. *Inorg. Chem.* **2025**, *64*, 3302–3310. [CrossRef]
42. Katz, M.J.; Brown, Z.J.; Colón, Y.J.; Siu, P.W.; Scheidt, K.A.; Snurr, R.Q.; Hupp, J.T.; Farha, O.K. A facile synthesis of UiO-66, UiO-67 and their derivatives. *Chem. Commun.* **2013**, *49*, 9449–9451. [CrossRef] [PubMed]
43. Valizadeh, B.; Nguyen, T.N.; Stylianou, K.C. Shape engineering of metal–organic frameworks. *Polyhedron* **2018**, *145*, 1–15. [CrossRef]
44. Mottillo, C.; Friščić, T. Advances in solid-state transformations of coordination bonds: From the ball mill to the aging chamber. *Molecules* **2017**, *22*, 144. [CrossRef] [PubMed]
45. Faustini, M.; Kim, J.; Jeong, G.-Y.; Kim, J.Y.; Moon, H.R.; Ahn, W.-S.; Kim, D.-P. Microfluidic approach toward continuous and ultrafast synthesis of metal–organic framework crystals and hetero structures in confined microdroplets. *J. Am. Chem. Soc.* **2013**, *135*, 14619–14626. [CrossRef]
46. Ntouros, V.; Kousis, I.; Pisello, A.L.; Assimakopoulos, M.N. Binding materials for MOF monolith shaping processes: A review towards real life application. *Energies* **2022**, *15*, 1489. [CrossRef]
47. Cohen, S.M. Postsynthetic methods for the functionalization of metal–organic frameworks. *Chem. Rev.* **2012**, *112*, 970–1000. [CrossRef]
48. Wang, Z.; Cohen, S.M. Postsynthetic modification of metal–organic frameworks. *Chem. Soc. Rev.* **2009**, *38*, 1315–1329. [CrossRef]
49. Lorignon, F.; Gossard, A.; Carboni, M. Hierarchically porous monolithic MOFs: An ongoing challenge for industrial-scale effluent treatment. *Chem. Eng. J.* **2020**, *393*, 124765. [CrossRef]
50. Thornton, A.W.; Babarao, R.; Jain, A.; Trousselet, F.; Coudert, F.-X. Defects in metal–organic frameworks: A compromise between adsorption and stability? *Dalton Trans.* **2016**, *45*, 4352–4359. [CrossRef]
51. Zhu, L.; Liu, X.-Q.; Jiang, H.-L.; Sun, L.-B. Metal–organic frameworks for heterogeneous basic catalysis. *Chem. Rev.* **2017**, *117*, 8129–8176. [CrossRef]
52. Liang, W.; Wied, P.; Carraro, F.; Sumby, C.J.; Nidetzky, B.; Tsung, C.K.; Falcaro, P.; Doonan, C.J. Metal-Organic Framework-Based Enzyme Biocomposites. *Chem. Rev.* **2021**, *121*, 1077–1129. [CrossRef]
53. Weng, Y.; Chen, R.; Hui, Y.; Chen, D.; Zhao, C.X. Boosting Enzyme Activity in Enzyme Metal-Organic Framework Composites. *Chem. Bio Eng.* **2024**, *1*, 99–112. [CrossRef]
54. Pelalak, R.; Thi, T.T.; Golestanifar, F.; Aallaei, M.; Heidari, Z. Molecular dynamics insights into the adsorption mechanism of acidic gases over iron based metal organic frameworks. *Sci. Rep.* **2025**, *15*, 21924. [CrossRef]
55. Jehanno, C.; Pérez-Madrigal, M.M.; Demarteau, J.; Sardon, H.; Dove, A.P. Organocatalysis for depolymerisation. *Polym. Chem.* **2019**, *10*, 172–186. [CrossRef]
56. Khopade, K.V.; Chikkali, S.H.; Barsu, N. Metal-catalyzed plastic depolymerization. *Cell Rep. Phys. Sci.* **2023**, *4*, 101341. [CrossRef]
57. Enache, A.-C.; Grecu, I.; Samoila, P. Polyethylene terephthalate (PET) recycled by catalytic glycolysis: A bridge toward circular economy principles. *Materials* **2024**, *17*, 2991. [CrossRef] [PubMed]
58. Javed, S.; Fisse, J.; Vogt, D. Optimization and kinetic evaluation for glycolytic depolymerization of post-consumer PET waste with sodium methoxide. *Polymers* **2023**, *15*, 687. [CrossRef]
59. Zhang, N.; Ding, M.; Yuan, Y. Current Advances in Biodegradation of Polyolefins. *Microorganisms* **2022**, *10*, 1537. [CrossRef]
60. Elora, A.A.; Sarker, T.; Tahmid, I.; Paul, P.; Moniruzzaman, M.; Ashaduzzaman, M.; Saha, B.B.; Sarker, M. Highly efficient $MnO_X/TiO_2$@ NH2-ZIF-8 composite for the removal of toxic textile dyes from water. *Colloids Surf. A Physicochem. Eng. Asp.* **2025**, *718*, 136882. [CrossRef]
61. Gracida-Alvarez, U.R.; Xu, H.; Benavides, P.T.; Wang, M.; Hawkins, T.R. Circular Economy Sustainability Analysis Framework for Plastics: Application for Poly(ethylene Terephthalate) (PET). *ACS Sustain. Chem. Eng.* **2023**, *11*, 514–524. [CrossRef]
62. Suo, Q.; Zi, J.; Bai, Z.; Qi, S. The glycolysis of poly (ethylene terephthalate) promoted by metal organic framework (MOF) catalysts. *Catal. Lett.* **2017**, *147*, 240–252. [CrossRef]
63. Han, N.; Lee, K.; Lee, J.; Jo, J.H.; An, E.J.; Lee, G.; Chi, W.S.; Lee, C. Dual-porous ZIF-8 heterogeneous catalysts with increased reaction sites for efficient PET glycolysis. *Chemosphere* **2024**, *364*, 143187. [CrossRef]

64. Yang, R.-X.; Bieh, Y.-T.; Chen, C.H.; Hsu, C.-Y.; Kato, Y.; Yamamoto, H.; Tsung, C.-K.; Wu, K.C.-W. Heterogeneous metal azolate framework-6 (MAF-6) catalysts with high zinc density for enhanced polyethylene terephthalate (PET) conversion. *ACS Sustain. Chem. Eng.* **2021**, *9*, 6541–6550. [CrossRef]
65. Wang, R.; Wang, T.; Yu, G.; Chen, X. A new class of catalysts for the glycolysis of PET: Deep eutectic solvent@ ZIF-8 composite. *Polym. Degrad. Stab.* **2021**, *183*, 109463. [CrossRef]
66. Xu, L.; Chen, Y.; Liu, Z.; Shao, Z.; Gao, F.; Gao, K.; Teng, C.; Zhang, L.; Xiao, P.; Song, G. Efficient alcoholysis of waste rigid polyurethane foam using MIL-101 (Fe) catalyst. *Sep. Purif. Technol.* **2025**, *366*, 132764. [CrossRef]
67. Liu, X.; Gao, C.; Sangwan, P.; Yu, L.; Tong, Z. Accelerating the degradation of polyolefins through additives and blending. *J. Appl. Polym. Sci.* **2014**, *131*, 40750. [CrossRef]
68. Chauhan, M.; Thadhani, C.; Rana, B.; Gupta, P.; Ghosh, B.; Manna, K. Hydrogenolysis of Polyethylene by Metal–Organic Framework Confined Single-Site Ruthenium Catalysts. *Chem. Mater.* **2024**, *36*, 10670–10679. [CrossRef]
69. Sun, S.; Huang, W. Chemical upcycling of polyolefin plastics using structurally well-defined catalysts. *JACS Au* **2024**, *4*, 2081–2098. [CrossRef]
70. Achilias, D.S. *Waste Material Recycling in the Circular Economy: Challenges and Developments*; BoD–Books on Demand: Norderstedt, Germany, 2022.
71. Sintim, H.Y.; Bary, A.I.; Hayes, D.G.; English, M.E.; Schaeffer, S.M.; Miles, C.A.; Zelenyuk, A.; Suski, K.; Flury, M. Release of micro-and nanoparticles from biodegradable plastic during in situ composting. *Sci. Total Environ.* **2019**, *675*, 686–693. [CrossRef]
72. Zhao, C.; Wu, J.; Gao, Y.; Zhou, J.; Zhang, L.; Wang, C.; Huo, Y.; Wang, X.; Huo, M. Optimizing Polylactic Acid Alcoholysis Efficiency with POM@ MOF Catalysis. *Colloids Surf. A Physicochem. Eng. Asp.* **2025**, *721*, 137192. [CrossRef]
73. Haider, T.P.; Völker, C.; Kramm, J.; Landfester, K.; Wurm, F.R. Plastics of the future? The impact of biodegradable polymers on the environment and on society. *Angew. Chem. Int. Ed.* **2019**, *58*, 50–62. [CrossRef]
74. Lithner, D.; Larsson, Å.; Dave, G. Environmental and health hazard ranking and assessment of plastic polymers based on chemical composition. *Sci. Total Environ.* **2011**, *409*, 3309–3324. [CrossRef] [PubMed]
75. Wang, J.; Liu, X.; Li, Y.; Powell, T.; Wang, X.; Wang, G.; Zhang, P. Microplastics as contaminants in the soil environment: A mini-review. *Sci. Total Environ.* **2019**, *691*, 848–857. [CrossRef] [PubMed]
76. Hahladakis, J.N.; Velis, C.A.; Weber, R.; Iacovidou, E.; Purnell, P. An overview of chemical additives present in plastics: Migration, release, fate and environmental impact during their use, disposal and recycling. *J. Hazard. Mater.* **2018**, *344*, 179–199. [CrossRef] [PubMed]
77. Ayanleye, S.O. Development of Preservative-Treated Cross-Laminated Timber and Lignin-Reinforced Polyurethane-Adhesive for Glued Laminated Timber. Ph.D. Thesis, Mississippi State University, Starkville, MS, USA, 2023.
78. Bócoli, P.F.J.; Gomes, V.E.d.S.; Maia, A.A.D.; Marangoni Júnior, L. Perspectives on Eco-Friendly Food Packaging: Challenges, Solutions, and Trends. *Foods* **2025**, *14*, 3062. [CrossRef]
79. Revel, M.; Châtel, A.; Mouneyrac, C. Micro (nano) plastics: A threat to human health? *Curr. Opin. Environ. Sci. Health* **2018**, *1*, 17–23. [CrossRef]
80. Emadian, S.M.; Onay, T.T.; Demirel, B. Biodegradation of bioplastics in natural environments. *Waste Manag.* **2017**, *59*, 526–536. [CrossRef]
81. Sánchez, M.; Duque, J.; Galindo, A.S.; Herrera, R.R. *Biodegradable Polymers*; CRC Press: Boca Raton, FL, USA, 2023.
82. Ren, J.; Dyosiba, X.; Musyoka, N.M.; Langmi, H.W.; Mathe, M.; Liao, S. Review on the current practices and efforts towards pilot-scale production of metal-organic frameworks (MOFs). *Coord. Chem. Rev.* **2017**, *352*, 187–219. [CrossRef]
83. Bagi, S.; Yuan, S.; Rojas-Buzo, S.; Shao-Horn, Y.; Román-Leshkov, Y. A continuous flow chemistry approach for the ultrafast and low-cost synthesis of MOF-808. *Green Chem.* **2021**, *23*, 9982–9991. [CrossRef]
84. McKinstry, C.; Cathcart, R.J.; Cussen, E.J.; Fletcher, A.J.; Patwardhan, S.V.; Sefcik, J. Scalable continuous solvothermal synthesis of metal organic framework (MOF-5) crystals. *Chem. Eng. J.* **2016**, *285*, 718–725. [CrossRef]
85. Rahman, R.; Malik, F.; Min Hein, Z.; Huang, J.; You, H.; Zhu, Y. Continuous Flow Synthesis and Applications of Metal-Organic Frameworks: Advances and Innovations. *ChemPlusChem* **2025**, *90*, e202400634. [CrossRef]
86. Bakuru, V.R.; Fazl-Ur-Rahman, K.; Periyasamy, G.; Velaga, B.; Peela, N.R.; DMello, M.E.; Kanakikodi, K.S.; Maradur, S.P.; Maji, T.K.; Kalidindi, S.B. Unraveling high alkene selectivity at full conversion in alkyne hydrogenation over Ni under continuous flow conditions. *Catal. Sci. Technol.* **2022**, *12*, 5265–5273. [CrossRef]
87. Swamy, A.; Kanakikodi, K.S.; Bakuru, V.R.; Kulkarni, B.B.; Maradur, S.P.; Kalidindi, S.B. Continuous Flow Liquid-Phase Semihydrogenation of Phenylacetylene over Pd Nanoparticles Supported on UiO-66 (Hf) Metal-Organic Framework. *ChemistrySelect* **2023**, *8*, e202203926. [CrossRef]
88. Chen, W.; Cai, P.; Elumalai, P.; Zhang, P.; Feng, L.; Al-Rawashdeh, M.m.; Madrahimov, S.T.; Zhou, H.-C. Site-isolated azobenzene-containing metal–organic framework for cyclopalladated catalyzed suzuki-miyuara coupling in flow. *ACS Appl. Mater. Interfaces* **2021**, *13*, 51849–51854. [CrossRef] [PubMed]

89. Thai, J.E.; Roach, M.C.; Reynolds, M.M. Continuous flow catalysis with CuBTC improves reaction time for synthesis of xanthene derivatives. *Front. Chem.* **2023**, *11*, 1259835. [CrossRef]
90. Griffiths, A.; Boyall, S.L.; Müller, P.; Harrington, J.P.; Sobolewska, A.M.; Reynolds, W.R.; Bourne, R.A.; Wu, K.; Collins, S.M.; Muldowney, M. MOF-based heterogeneous catalysis in continuous flow via incorporation onto polymer-based spherical activated carbon supports. *Nanoscale* **2023**, *15*, 17910–17921. [CrossRef]
91. Jia, J.; Yang, C.; Xu, F.; Xu, S.; Zhang, X. Metal organic frameworks as solid catalyst for flow acetalization of benzaldehyde. *Microchem. J.* **2021**, *165*, 106113. [CrossRef]
92. Hu, H.; Wu, S.; Zheng, Y.; Zhang, Z.; Yang, M.; Chen, Y. Dynamic exchange strategy for enzyme immobilization in Zr-based metal-organic frameworks for green synthesis of β-lactam antibiotics. *Green Chem. Eng.* **2025**. [CrossRef]
93. Patil, P.D.; Gargate, N.; Tiwari, M.S.; Nadar, S.S. Defect metal-organic frameworks (D-MOFs): An engineered nanomaterial for enzyme immobilization. *Coord. Chem. Rev.* **2025**, *531*, 216519. [CrossRef]
94. Ban, Y.; Cao, N.; Yang, W. Metal-organic framework membranes and membrane reactors: Versatile separations and intensified processes. *Research* **2020**, *2020*, 1583451. [CrossRef]
95. Zheng, W.; Lee, L.Y.S. Metal–Organic Frameworks for Electrocatalysis: Catalyst or Precatalyst? *ACS Energy Lett.* **2021**, *6*, 2838–2843. [CrossRef]
96. Sanati, S.; Morsali, A.; Garcia, H. Metal-organic framework-based materials as key components in electrocatalytic oxidation and reduction reactions. *J. Energy Chem.* **2023**, *87*, 540–567. [CrossRef]
97. McCarthy, B.D.; Beiler, A.M.; Johnson, B.A.; Liseev, T.; Castner, A.T.; Ott, S. Analysis of electrocatalytic metal-organic frameworks. *Coord. Chem. Rev.* **2020**, *406*, 213137. [CrossRef]
98. Escobar-Hernandez, H.U.; Quan, Y.; Papadaki, M.I.; Wang, Q. Life cycle assessment of metal–organic frameworks: Sustainability study of zeolitic imidazolate framework-67. *ACS Sustain. Chem. Eng.* **2023**, *11*, 4219–4225. [CrossRef]
99. Grande, C.A.; Blom, R.; Spjelkavik, A.; Moreau, V.; Payet, J. Life-cycle assessment as a tool for eco-design of metal-organic frameworks (MOFs). *Sustain. Mater. Technol.* **2017**, *14*, 11–18. [CrossRef]
100. Singh, A.; Rorrer, N.A.; Nicholson, S.R.; Erickson, E.; DesVeaux, J.S.; Avelino, A.F.; Lamers, P.; Bhatt, A.; Zhang, Y.; Avery, G. Techno-economic, life-cycle, and socioeconomic impact analysis of enzymatic recycling of poly (ethylene terephthalate). *Joule* **2021**, *5*, 2479–2503. [CrossRef]
101. Chu, J.; Ke, F.-S.; Wang, Y.; Feng, X.; Chen, W.; Ai, X.; Yang, H.; Cao, Y. Facile and reversible digestion and regeneration of zirconium-based metal-organic frameworks. *Commun. Chem.* **2020**, *3*, 5. [CrossRef] [PubMed]
102. Wu, Z.; Yu, Y.; Chen, J.; Liu, Y.; Zou, C. The impact of metal leaching in MOF materials on the evaluation of photocatalytic $CO_2$ reduction activity—A case study. *Next Energy* **2025**, *7*, 100296. [CrossRef]
103. Yang, D.; Gates, B.C. Catalysis by metal organic frameworks: Perspective and suggestions for future research. *ACS Catal.* **2019**, *9*, 1779–1798. [CrossRef]
104. Waribam, P.; Katugampalage, T.R.; Opaprakasit, P.; Ratanatawanate, C.; Chooaksorn, W.; Wang, L.P.; Liu, C.-H.; Sreearunothai, P. Upcycling plastic waste: Rapid aqueous depolymerization of PET and simultaneous growth of highly defective UiO-66 metal-organic framework with enhanced $CO_2$ capture via one-pot synthesis. *Chem. Eng. J.* **2023**, *473*, 145349. [CrossRef]
105. Wan, Y.; Kong, D.; Xiong, F.; Qiu, T.; Gao, S.; Zhang, Q.; Miao, Y.; Qin, M.; Wu, S.; Wang, Y. Enhancing hydrophobicity via core–shell metal organic frameworks for high-humidity flue gas $CO_2$ capture. *Chin. J. Chem. Eng.* **2023**, *61*, 82–89. [CrossRef]
106. Joseph, L.; Jun, B.-M.; Jang, M.; Park, C.M.; Muñoz-Senmache, J.C.; Hernández-Maldonado, A.J.; Heyden, A.; Yu, M.; Yoon, Y. Removal of contaminants of emerging concern by metal-organic framework nanoadsorbents: A review. *Chem. Eng. J.* **2019**, *369*, 928–946. [CrossRef]
107. Canivet, J.; Fateeva, A.; Guo, Y.; Coasne, B.; Farrusseng, D. Water adsorption in MOFs: Fundamentals and applications. *Chem. Soc. Rev.* **2014**, *43*, 5594–5617. [CrossRef] [PubMed]
108. Férey, G.; Serre, C.; Devic, T.; Maurin, G.; Jobic, H.; Llewellyn, P.L.; De Weireld, G.; Vimont, A.; Daturi, M.; Chang, J.-S. Why hybrid porous solids capture greenhouse gases? *Chem. Soc. Rev.* **2011**, *40*, 550–562. [CrossRef] [PubMed]
109. Du, C.; Xu, Y.; Wei, G. Recent Advances in Biomolecule-Engineered Metal-Organic Frameworks (Bio-MOFs): From Design, Bioengineering, and Structural/functional Regulation to Biocatalytic Applications. *Chem. Rec.* **2025**, *25*, e202500001. [CrossRef]
110. Hu, Z.; Deibert, B.J.; Li, J. Luminescent metal–organic frameworks for chemical sensing and explosive detection. *Chem. Soc. Rev.* **2014**, *43*, 5815–5840. [CrossRef]
111. Lin, S.; Diercks, C.S.; Zhang, Y.-B.; Kornienko, N.; Nichols, E.M.; Zhao, Y.; Paris, A.R.; Kim, D.; Yang, P.; Yaghi, O.M. Covalent organic frameworks comprising cobalt porphyrins for catalytic $CO_2$ reduction in water. *Science* **2015**, *349*, 1208–1213. [CrossRef]
112. Jiao, L.; Wang, Y.; Jiang, H.L.; Xu, Q. Metal–organic frameworks as platforms for catalytic applications. *Adv. Mater.* **2018**, *30*, 1703663. [CrossRef]
113. Li, Z.; Peters, A.W.; Bernales, V.; Ortuno, M.A.; Schweitzer, N.M.; DeStefano, M.R.; Gallington, L.C.; Platero-Prats, A.E.; Chapman, K.W.; Cramer, C.J. Metal–organic framework supported cobalt catalysts for the oxidative dehydrogenation of propane at low temperature. *ACS Cent. Sci.* **2017**, *3*, 31–38. [CrossRef]

114. Rösler, C.; Fischer, R.A. Metal–organic frameworks as hosts for nanoparticles. *CrystEngComm* **2015**, *17*, 199–217. [CrossRef]
115. Dissegna, S.; Epp, K.; Heinz, W.R.; Kieslich, G.; Fischer, R.A. Defective metal-organic frameworks. *Adv. Mater.* **2018**, *30*, 1704501. [CrossRef]
116. Fang, Z.; Bueken, B.; De Vos, D.E.; Fischer, R.A. Defect-engineered metal–organic frameworks. *Angew. Chem. Int. Ed.* **2015**, *54*, 7234–7254. [CrossRef]
117. Lu, W.; Wei, Z.; Gu, Z.-Y.; Liu, T.-F.; Park, J.; Park, J.; Tian, J.; Zhang, M.; Zhang, Q.; Gentle III, T. Tuning the structure and function of metal–organic frameworks via linker design. *Chem. Soc. Rev.* **2014**, *43*, 5561–5593. [CrossRef]
118. Sun, D.; Fu, Y.; Liu, W.; Ye, L.; Wang, D.; Yang, L.; Fu, X.; Li, Z. Studies on photocatalytic $CO_2$ reduction over NH2-Uio-66 (Zr) and its derivatives: Towards a better understanding of photocatalysis on metal–organic frameworks. *Chem.—A Eur. J.* **2013**, *19*, 14279–14285. [CrossRef]
119. Jabbour, C. Synthesis, Characterization, and Shaping of UiO-67 Metal-Organic Frameworks. Ph.D. Thesis, Utrecht University, Utrecht, New Zealand, 2024.
120. Nguyen, C.T.; Tec-Caamal, E.N.; Natarajan, A.; Thanh, N.C. New strategies and advancements in the synthesis of metal organic frameworks for PAHs removal. *iScience* **2025**, *28*, 112561. [CrossRef]
121. Choi, K.M.; Kim, D.; Rungtaweevoranit, B.; Trickett, C.A.; Barmanbek, J.T.D.; Alshammari, A.S.; Yang, P.; Yaghi, O.M. Plasmon-enhanced photocatalytic $CO_2$ conversion within metal–organic frameworks under visible light. *J. Am. Chem. Soc.* **2017**, *139*, 356–362. [CrossRef]
122. Zhang, X.; Chen, Z.; Liu, X.; Hanna, S.L.; Wang, X.; Taheri-Ledari, R.; Maleki, A.; Li, P.; Farha, O.K. A historical overview of the activation and porosity of metal–organic frameworks. *Chem. Soc. Rev.* **2020**, *49*, 7406–7427. [CrossRef] [PubMed]
123. Cai, G.; Yan, P.; Zhang, L.; Zhou, H.-C.; Jiang, H.-L. Metal–organic framework-based hierarchically porous materials: Synthesis and applications. *Chem. Rev.* **2021**, *121*, 12278–12326. [CrossRef] [PubMed]
124. Julien, P.A.; Mottillo, C.; Friščić, T. Metal–organic frameworks meet scalable and sustainable synthesis. *Green Chem.* **2017**, *19*, 2729–2747. [CrossRef]
125. Rubio-Martinez, M.; Avci-Camur, C.; Thornton, A.W.; Imaz, I.; Maspoch, D.; Hill, M.R. New synthetic routes towards MOF production at scale. *Chem. Soc. Rev.* **2017**, *46*, 3453–3480. [CrossRef]
126. Zhou, H.-C.; Long, J.R.; Yaghi, O.M. Introduction to metal–organic frameworks. *Chem. Rev.* **2012**, *112*, 673–674. [CrossRef]
127. Cohen, S.M. Modifying MOFs: New chemistry, new materials. *Chem. Sci.* **2010**, *1*, 32–36. [CrossRef]
128. Evans, J.D.; Coudert, F.-X. Predicting the mechanical properties of zeolite frameworks by machine learning. *Chem. Mater.* **2017**, *29*, 7833–7839. [CrossRef]
129. Rahmah, W.; Khoiruddin, K.; Wenten, I.G.; Kawi, S. Advancing Carbon Capture with Bio-Inspired Membrane Materials: A review. *Carbon Capture Sci. Technol.* **2024**, *13*, 100318. [CrossRef]


**Disclaimer/Publisher's Note:** The statements, opinions and data contained in all publications are solely those of the individual author(s) and contributor(s) and not of MDPI and/or the editor(s). MDPI and/or the editor(s) disclaim responsibility for any injury to people or property resulting from any ideas, methods, instructions or products referred to in the content.